Numerical Resolution of a Multiphasic Optimal Mass Transport Problem

Jean-David Benamou, Yann Brenier, Kevin Guittet

INRIA

INSTITUT NATIONAL DE RECHERCHE EN INFORMATIQUE ET EN AUTOMATIQUE

Numerical Resolution of a Multiphasic Optimal Mass Transport Problem

Jean-David Benamou , Yann Brenier , Kévin Guittet

N ° 4022

Octobre 2000

THÈME 4

ISSN 0249-6399 ISRN INRIA/RR--4022--FR+ENG

INRIA
ROCQUENCOURT

Numerical Resolution of a Multiphasic Optimal Mass Transport Problem

Jean-David Benamou * , Yann Brenier † , Kévin Guittet ‡

Thème 4 — Simulation et optimisation
de systèmes complexes
Projet Ondes

Rapport de recherche n ° 4022 — Juin 2000 — pages

Abstract: We extend the classical L^2 Monge-Kantorovich Problem in the multiphasic context. An augmented lagrangian numerical method used in the monophasic case is adapted to this problem, its efficiency being checked with various methods.

(Résumé : tsvp)

* INRIA, Domaine de Voluceau, B.P.105 78153 Le Chesnay cedex, France, e-mail :Jean-David.Benamou@inria.fr

† Laboratoire d'analyse numérique, Université Paris 6, 4 place Jussieu, 75752 Paris cedex 05, France. e-mail :Brenier@ann.jussieu.fr

‡ Ecole Normale Supérieure, 45, rue d'Ulm , 75005 Paris, France, e-mail :guittet@clipper.ens.fr

Unité de recherche INRIA Rocquencourt
Domaine de Voluceau, Rocquencourt, BP 105, 78153 LE CHESNAY Cedex (France)
Téléphone : 01 39 63 55 11 - International : +33 1 39 63 55 11
Télécopie : (33) 01 39 63 53 30 - International : +33 1 39 63 53 30

Résolution numérique d'un problème de transport optimal de masse à plusieurs phases

Résumé : Ce rapport présente le problème de transport de masse à plusieurs phases, avec une densité totale fixée. La méthode numérique de Lagrangien augmenté utilisée pour le cas monophasique est adaptée à la résolution de ce problème, et différentes vérifications sont effectuées.

We extend the classical L^2 Monge-Kantorovich Problem in the multiphasic context. An augmented lagrangian numerical method used in the monophasic case is adapted to this problem, its efficiency being checked with various methods.

1 Introduction

In [4], a numerical method to solve the following mass transport problem :

Given two bounded, positive mesurable functions ρ_0 and ρ_T with same mass in the torus $D = \mathbb{R}^d/\mathbb{Z}^d$, find an application M wich realizes the transport from ρ_0 to ρ_T in the following sense : For all borel set A, M satisfyes

$$\int_{M^{-1}(A)} \rho_0(x)dx = \int_A \rho_T(x)dx \ , \tag{1}$$

and achieves the minimal cost

$$\int_D |x - M(x)|^2 \rho_0(x)dx \ . \tag{2}$$

The minimal cost is the wasserstein metric between ρ_0 and ρ_T. In order to compute this optimal map, a time-continuous reformulation of the problem was introduced. The numerical method hang on the following result :

Theorem 1.1. *The square of the Wasserstein distance is equal to :*

$$\inf_{(\rho,v)} T \int_{\mathbb{R}^d} \int_0^T \rho(t,x)|v(t,x)|^2 dxdt, \tag{3}$$

where the time horizon $T > 0$ is arbitrarily fixed and the infimum is performed over all pair $\rho(t,x) \geq 0$ $v(t,x) \in \mathbb{R}^d$ of density and velocity fields satisfying the conservation law

$$\partial_t \rho + \nabla.(\rho v) = 0 \tag{4}$$

for $0 < t < T$ and $x \in \mathbb{R}^d$, and subject to the initial and final conditions

$$\rho(0,.) = \rho_0, \ \ \rho(T,.) = \rho_T. \tag{5}$$

The time-continuous formulation however can be extended in a multiphasic context : as in the monophasic case, we know the initial and final densities, but we also precisely know the evolution of the global density. Then the problem is to determine the intermediary states of the system.

More concretely, we have to minimize the kinetic energy

$$K(\rho, v) = \frac{1}{2} \sum_{\alpha=1}^{M} \mu_\alpha \int_0^T \int_D \rho_\alpha(t,x)|v_\alpha(t,x)|^2 dxdt \tag{6}$$

in the class of functions such that :

$$0 \leq \rho_\alpha \in L^\infty(Q),\ m_\alpha = \rho_\alpha v_\alpha,\ v_\alpha \in L^2(Q, \rho_\alpha dt\ dx), \tag{7}$$

$$\sum_{\alpha=1}^{M} \rho_\alpha = \bar{\rho},\ \partial_t \rho_\alpha + \nabla . m_\alpha = 0, \tag{8}$$

$$\rho_\alpha(0,.) = \rho_\alpha^0,\ \rho_\alpha(T,.) = \rho_\alpha^T \tag{9}$$

Let us consider time boundary data $(\rho_\alpha^0, \rho_\alpha^T)$ defined a.e. on D with non-negative values, and a fixed global density $\bar{\rho}$ satisfying the compatibility conditions :

$$\sum_{\alpha=1}^{M} \rho_\alpha^0(.) = \bar{\rho}(0,.),\ \sum_{\alpha=1}^{M} \rho_\alpha^T(.) = \bar{\rho}(T,.)\ , \tag{10}$$

$$\forall \alpha \in [0;\alpha], \int_D \rho_\alpha^0(.) = \int_D \rho_\alpha^T(.)\ , \tag{11}$$

$$\forall t \in [0;T],\ \sum_{\alpha=1}^{M} \int_D \rho_\alpha^0(.) = \int_D \bar{\rho}(t,.)\ . \tag{12}$$

and set

$$I(\rho_0, \rho_T) = \inf K(\rho, v) \tag{13}$$

for (ρ_α, v_α) such that (7), (8) and (9) hold.

When there is only one phase (i.e. $M = 1$), and if we remove the condition on the global density, we recover the time-continuous Monge Transport problem. It can be of interest to study how the constraint on the globlal density acts on the behaviour of the system. For this purpose, we only consider the monodimensional case of the translation of a step.

In the first example, we consider two phases such that the global density is a constant for the initial and final times, but without constraint (8). That is there are two phases, which do not see each other. The red line on figure 1 shows the evolution of the first density, while the blue line shows the evolution of the global density. We see that the densities translate from the initial to the final states.

In the second example, we consider two phases such that the global density is always a constant. On the results shown in figure 2, we see how the phases cross under the incompressibility constraint.

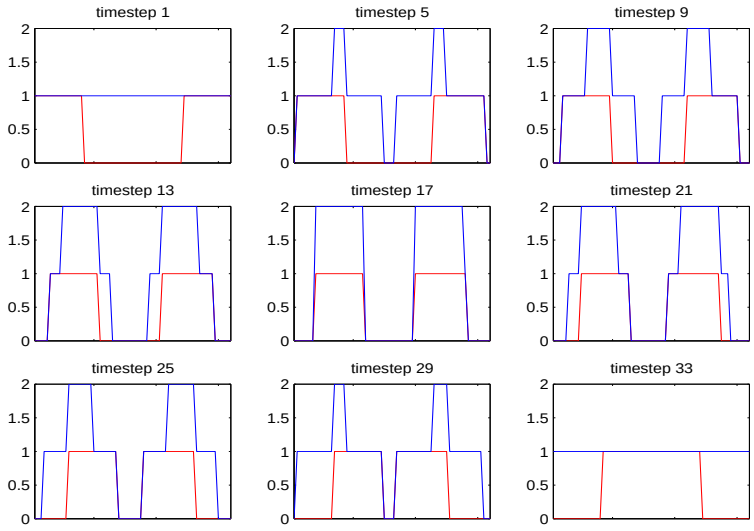

Figure 1: Monophasic-style step translation

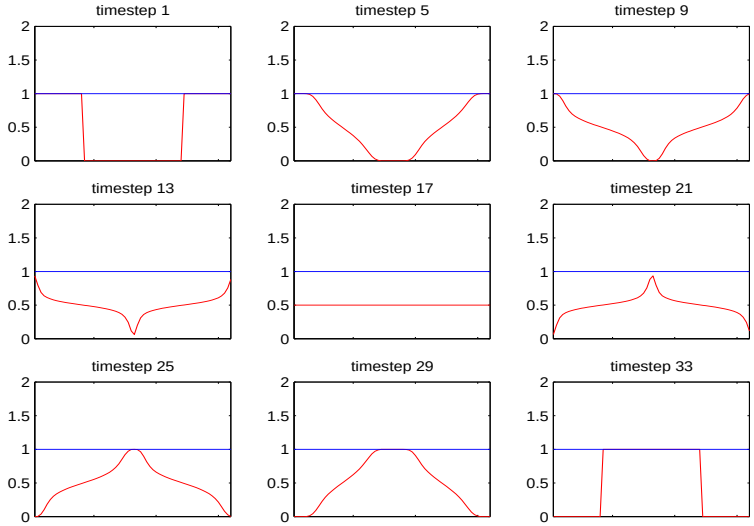

Figure 2: Biphasic step translation

Moreover, the incompressibility constraint acts on the trajectories of the fluid particles. The trajectories $X(t,x)$ are the integral curves of the velocity :

$$\begin{cases} \partial_t X(t,x) = v(t, X(t,x)) \ , \\ \\ X(0,x) = x \ . \end{cases} \tag{14}$$

In the monophasic-style case, the particle have a constant velocity, but in the biphasic case, it is not true anymore. The presented results are one dimensional, but in higher dimension, the trajectories can even show some curvature effects. Figures 3 and 4 allow a visual comparison of the trajectories in both examples.

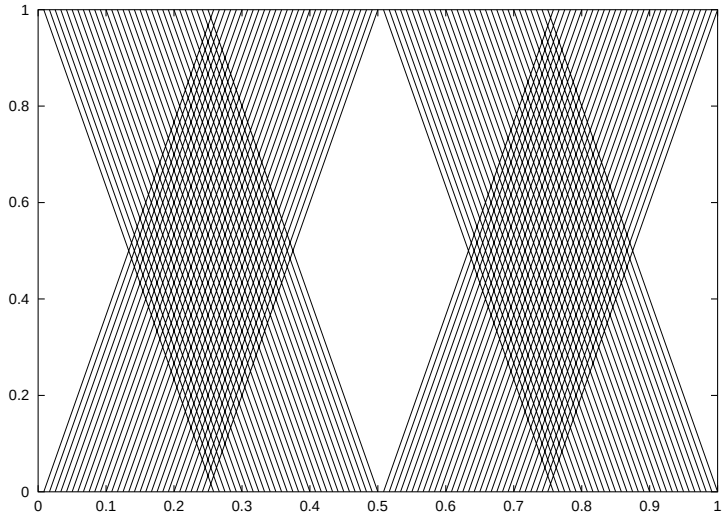

Figure 3: Monophasic-style trajectories

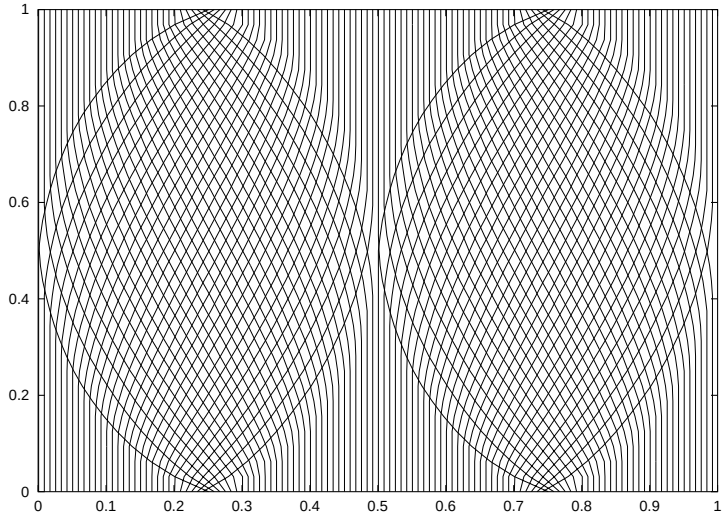

Figure 4: Biphasic trajectories

But the multiphasic case shows interesting properties in itself. Indeed, the condition on the global density acts as an incompressibility constraint, and his associated lagrange multiplier is the pressure. The formal optimality conditions on the lagrangian of the problem are :

$$v_\alpha = \nabla_x \phi_\alpha \qquad \text{in }]0,T[\times D\ , \tag{15}$$

$$\partial_t \phi_\alpha + \frac{|\nabla_x \phi_\alpha|^2}{2} + \frac{p}{\mu_\alpha} = 0 \qquad \text{in }]0,T[\times D\ , \tag{16}$$

$$\partial_t \rho_\alpha + \nabla.(\rho_\alpha \nabla_x \phi_\alpha) = 0 \qquad \text{in }]0,T[\times D\ , \tag{17}$$

$$\rho_\alpha(0,.) = \rho_\alpha^0, \rho_\alpha(T,.) = \rho_\alpha^T \qquad \text{in } D\ , \tag{18}$$

$$\sum_{\alpha=1}^{M} \rho_\alpha(t,x) = \bar{\rho}(t,x) \qquad \text{in }]0,T[\times D\ . \tag{19}$$

Taking $\bar{\rho} = 1$ and $\mu_\alpha = 1$ for every α, we recognize the "homogenized vortex-sheet equations". Those equations have been studied in [5], and we can deduce from Brenier's work the following existence theorem :

Theorem 1.2. *There exists $(\rho_\alpha, m_\alpha = \rho_\alpha v_\alpha)$ satisfying (7) and (8), and for each $\epsilon > 0$, functions $\phi_{\alpha\epsilon} \in C^1(\bar{Q})$, $p_\epsilon \in C^0(\bar{Q})$ such that*

$$\int_Q \rho_\alpha |v_\alpha - \nabla \phi_{\alpha\epsilon}|^2 dxdt \leq \epsilon\ , \tag{20}$$

$$\int_Q \rho_\alpha |\partial_t \phi_{\alpha\epsilon} + \frac{1}{2}|\nabla \phi_{\alpha\epsilon}|^2 + \frac{p_\epsilon}{\mu_\alpha}|^2 dxdt \leq \epsilon\ , \tag{21}$$

$$\partial_t \phi_{\alpha\epsilon} + \frac{1}{2}|\nabla \phi_{\alpha\epsilon}|^2 + \frac{p_\epsilon}{\mu_\alpha} \leq \epsilon\ , \tag{22}$$

$$K(\rho, v) = I(\rho_0, \rho_T)\ . \tag{23}$$

(ρ_α, m_α) is called a "variational solution" of equations (8), (16).

Once the problem is known to have a solution, the question moves to the computation of this solution. This is the purpose of the following section.

2 The numerical method

The following compact notations are used throughout this section :

- $D = \mathbb{R}^d/\mathbb{Z}^d$ is the periodic unit cube, $[0,T]$ is a fixed time interval.
- ∇_x is the spatial gradient in $\mathbb{R}^d$.
- Δ_x is the spatial Laplacian in $\mathbb{R}^d$.
- ∂_t is the time derivative.
- . and $|.|$ denote the inner product and the Euclidean norm in $\mathbb{R}^d$.
- $\nabla_{t,x} = \{\partial_t, \nabla_x\}$ is the time-space gradient in $\mathbb{R} \times \mathbb{R}^d$.
- $\Delta_{t,x} = \partial_{t^2} + \Delta_x$ is the time-space Laplacian in $\mathbb{R} \times \mathbb{R}^d$.
- For two vectors in $\mathbb{R} \times \mathbb{R}^d$, a, b and a', b', $\{a,b\}.\{a',b'\} = aa' + b.b'$ denotes the inner product.

2.1 The Lagrangian

We use the Lagrangian formulation of the multiphasic optimal time-continuous mass transport problem now set on the periodic domain D. The Lagrangian is given by :

$$\begin{aligned} L(\rho_\alpha, m_\alpha, \phi_\alpha, p) &= \sum_{\alpha=1}^{M} \mu_\alpha \int_0^T \int_D -\rho_\alpha \partial_t \phi_\alpha - m_\alpha . \nabla_x \phi_\alpha + \frac{|m_\alpha(t,x)|^2}{2\rho_\alpha(t,x)} dxdt \\ &\quad - \sum_{\alpha=1}^{M} \mu_\alpha \int_D [\rho_\alpha^0 \phi(0,.) - \rho_\alpha^T \phi(T,.)]dx \\ &\quad + \int_0^T \int_D [\bar{\rho}(t,x) - \sum_{\alpha=1}^{M} \rho_\alpha(t,x)] p(t,x) dxdt \ , \end{aligned} \tag{24}$$

where the ϕ_α and p are the lagrange multipliers of constraints (8).

We are then led to solve the following problem :

$$\inf_{(\rho_\alpha, m_\alpha)} \sup_{(\phi_\alpha, p)} L(\rho_\alpha, m_\alpha, \phi_\alpha, p) \tag{25}$$

The (formal) optimality conditions for this problem are :

$$\begin{cases} \partial_t \phi_\alpha + \dfrac{|m_\alpha|^2}{2\rho_\alpha^2} + \dfrac{p}{\mu_\alpha} = 0 & \text{in }]0,T[\times D\ , \\ \dfrac{m_\alpha}{\rho_\alpha} = \nabla_x \phi_\alpha & \text{in }]0,T[\times D\ , \\ \partial_t \rho_\alpha + \nabla_x . m_\alpha = 0 & \text{in }]0,T[\times D\ , \\ \rho_\alpha(0,.) = \rho_\alpha^0, \rho_\alpha(T,.) = \rho_\alpha^T & \text{in } D\ , \\ \sum_{\alpha=1}^{M} \rho_\alpha(t,x) = \bar{\rho}(t,x) & \text{in }]0,T[\times D\ . \end{cases} \tag{26}$$

We notice that m can be eliminated, and then recover the optimality conditions introduced in the previous section :

$$\begin{cases} \partial_t \phi_\alpha + \dfrac{|\nabla_x \phi_\alpha|^2}{2} + \dfrac{p}{\mu_\alpha} = 0 & \text{in }]0,T[\times D\ , \\ \partial_t \rho_\alpha + \nabla . (\rho_\alpha \nabla_x \phi_\alpha) = 0 & \text{in }]0,T[\times D\ , \\ \rho_\alpha(0,.) = \rho_\alpha^0, \rho_\alpha(T,.) = \rho_\alpha^T & \text{in } D\ , \\ \sum_{\alpha=1}^{M} \rho_\alpha(t,x) = \bar{\rho}(t,x) & \text{in }]0,T[\times D\ . \end{cases} \tag{27}$$

2.2 Reformulation.

In this section, we reformulate the problem using the terminology of [23]. We therefore use the following characterization introduced in [3], which is that, for positive ρ, we have :

$$\frac{|m|^2}{2\rho} = \sup_{a + \frac{|b|^2}{2} \leq 0} [a\rho + b.m] \tag{28}$$

We then easily get

Lemma 2.1. *Using the following variables and notations :*

$$\begin{cases} l_\alpha = \{\rho_\alpha, m_\alpha\} \\ q_\alpha = \{a_\alpha, b_\alpha\} \\ \tilde{p}_\alpha = \frac{1}{\mu_\alpha}\{p, 0\} \\ F(q) = \begin{cases} 0 \ \textit{if } q \in K \\ +\infty \ \textit{else} \end{cases} \\ G(\phi) = \int_D [\phi(0,.)\rho_0 - \phi(T,.)\rho_T] \\ H(p) = \int_0^T \int_D \bar{\rho} p \\ < l, q >= \int_0^T \int_D \mu_\alpha l_\alpha . q_\alpha\ , \end{cases} \tag{29}$$

we can write problem (25) as :

$$\sup_{l} \inf_{\phi,q,p} [F(q) + G(\phi) + H(p) + < l, \nabla_{t,x}\phi + \tilde{p} - q >]\ . \tag{30}$$

Taking $\chi = (\phi, \tilde{p})$ as a single variable and then denoting $B(\chi) = \nabla_{t,x}\phi + \tilde{p}$, we get :

$$\sup_{l} \inf_{\chi,q} [F(q) + G(\chi) + < l, B(\chi) - q >] . \tag{31}$$

Such Lagrangian formulations are used in [23] for solving problems of the form

$$\min_{v} \{F(Bv) + G(v)\} ,$$

where F, G are convex functionals and B is a linear operator.

In order to fully comply with the hypothesis on F, G, and B used in [23], F has to be strictly coercive, and B has to be injective with a closed range.

1. We lack coercivity on F. A simple way to fix this problem is to replace F by the perturbed function F_{ϵ_1} :

   $$F_{\epsilon_1}(q) = F(q) + \epsilon_1 < q, q > .$$

   We should mention that, in practice, we obtain fully satisfactory results just with $\epsilon_1 = 0$. This will also be discussed later.

2. Since the calculations are performed in a finite dimensional space, B always has a closed range.

3. We want to have an injective B. In fact, we can always choose ϕ modulo a suitable additive constant, such that B is injective.

2.3 The augmented lagrangian and the numerical method ALG2

In this section,we simply apply the augmented Lagrangian technique of [23] (chapter 3). First, we define the "augmented" Lagrangian :

$$\begin{aligned} L_r(\phi, p, q, l) = \quad & F_{\epsilon_1}(q) + G(\phi) + < l, \nabla_{t,x}\phi + \tilde{p} - q > \\ & + \tfrac{r}{2} < \nabla_{t,x}\phi + \tilde{p} - q, \nabla_{t,x}\phi + \tilde{p} - q > , \end{aligned} \tag{32}$$

where r is a positive parameter.

Then, a simple algorithm, called ALG2, based on relaxations of the Uzawa algorithm is proposed to solve the problem :

$$\sup_{l} \inf_{\phi,p,q} L_r(\phi, p, q, l). \tag{33}$$

We detail below the algorithm. It is a three step iterative method which constructs a sequence (ϕ^n, p^n, q^n, l^n) converging to the saddle point.

ALG2:

- $(\phi^{n-1}, p^{n-1}, q^{n-1}, l^n)$ are given.
- Step A: Find (ϕ^n, p^n) such that :

$$L_r(\phi^n, p^n, q^n, l^n) \leq L_r(\phi, p, q^{n-1}, l^n), \ \ \forall(\phi, p). \tag{34}$$

- Step B: Find q^n such that :

$$L_r(\phi^n, p^n, q^n, l^n) \leq L_r(\phi^n, p^n, q, l^n), \ \ \forall q. \tag{35}$$

- Step C : Do

$$l_\alpha^{n+1} = l_\alpha^n + \delta^n(\nabla_{t,x}\phi_\alpha^n - q_\alpha^n + \tilde{p}_\alpha^n) \tag{36}$$

  (where $\delta^n > 0$ is a parameter, wich can be taken equal to r, the parameter of the Augmented Lagrangian).

- Go back to step A.

Step A and B are simply a relaxation method for the minimization part of the saddle point problem. Step C is a gradient step for the dual problem.

2.4 Interpretation of the method

We now interpret each of these steps in terms of our functions F and G.

2.4.1 Step A

We notice that the first step is a minimization on both ϕ_α and p, that is a minimization on the variable χ. This is possible thanks to the fact that p can be expressed in term of ϕ. Indeed, if we first check the optimality condition in p, we get :

$$[\bar{\rho} - \sum_{\alpha=1}^{M} \rho_\alpha] + r \sum_{\alpha=1}^{M} (a_\alpha - \partial_t \phi_\alpha - \frac{p}{\mu_\alpha}) = 0 \tag{37}$$

We then deduce that :

$$p = \frac{1}{\sum_{\alpha=1}^{M} \frac{1}{\mu_\alpha}} (\frac{1}{r}[\bar{\rho} - \sum_{\alpha=1}^{M} \rho_\alpha] + \sum_{\alpha=1}^{M} [a_\alpha - \partial_t \phi_\alpha]) \tag{38}$$

The optimality condition in ϕ in given by the differentiation of L_r in ϕ. We should have :

$$
\begin{aligned}
0 \;=\; & \sum_{\alpha=1}^{M} \mu_\alpha \int_0^T \int_D (-\partial_t \tilde{\phi}_\alpha)\rho_\alpha - \nabla\tilde{\phi}_\alpha . m_\alpha dxdt \\
& - \sum_{\alpha=1}^{M} \mu_\alpha \int_D [\rho_\alpha^0 \tilde{\phi}(0,.) - \rho_\alpha^T \tilde{\phi}(T,.)]dx \\
& + r\sum_{\alpha=1}^{M} \mu_\alpha \int_0^T \int_D [a_\alpha - \partial_t\phi_\alpha - \frac{p}{\mu_\alpha}]\partial_t\tilde{\phi}_\alpha dxdt \\
& + r\sum_{\alpha=1}^{M} \mu_\alpha \int_0^T \int_D (b_\alpha - \nabla\phi_\alpha).\nabla\tilde{\phi}_\alpha dxdt
\end{aligned}
\tag{39}
$$

Injecting the value of p, notating $\Gamma = \sum_{\alpha=1}^{M} \frac{1}{\mu_\alpha}$, and then integrating by parts with periodic boundary conditions, we get :

$$
\begin{aligned}
r\mu_\alpha \Delta_{t,x}\phi_\alpha - \frac{r}{\Gamma}\sum_{\alpha'=1}^{M} \partial_{tt}\phi_{\alpha'} &= \mu_\alpha \partial_t(ra_\alpha - \rho_\alpha) - \frac{1}{\Gamma}\partial_t\bar{\rho} \\
-\frac{1}{\Gamma}\sum_{\alpha'=1}^{M} \partial_t(ra_{\alpha'} - \rho_{\alpha'}) + \mu_\alpha \nabla.(rb_\alpha - m_\alpha) &\;,
\end{aligned}
\tag{40}
$$

with the following boundary conditions in time :

$$
\left\{
\begin{array}{rcl}
\mu_\alpha \partial_t\phi_\alpha(0,.) & = & -\mu_\alpha([\rho_\alpha(0,.) - \rho_\alpha^0] - ra_\alpha(0,.)) \\
& & -\frac{1}{\Gamma}\sum_{\alpha'=1}^{M} r[a_{\alpha'} - \partial_t\phi_{\alpha'}](0,.) - \frac{1}{\Gamma}[\bar{\rho} - \sum_{\alpha'=1}^{M} \rho_{\alpha'}](0,.) \;, \\
\mu_\alpha \partial_t\phi_\alpha(T,.) & = & -\mu_\alpha([\rho_\alpha(T,.) - \rho_\alpha^T] - ra_\alpha(T,.)) \\
& & -\frac{1}{\Gamma}\sum_{\alpha'=1}^{M} r[a_{\alpha'} - \partial_t\phi_{\alpha'}](T,.) - \frac{1}{\Gamma}[\bar{\rho} - \sum_{\alpha'=1}^{M} \rho_{\alpha'}](T,.) \;.
\end{array}
\right.
\tag{41}
$$

We see that we have a differential operator denoted by L :

$$
\forall \phi,\; L(\phi)_\alpha = \mu_\alpha \Delta_{t,x}\phi_\alpha - \frac{1}{\Gamma}\sum_{\alpha'=1}^{M} \partial_{tt}\phi_{\alpha'} \;. \tag{42}
$$

Since we want to solve this system, it's of primary importance to see wether this system is of elliptic type or not. Computing $I(\phi) =< L(\phi), \phi >$ for any $\phi \in H_0^1(D \times [0;t])^M$, we get

$$I(\phi) \leq -\sum_{\alpha=1}^{M} \mu_\alpha \|\nabla_x \phi_\alpha\|_{L^2}^2 \ .$$

This is not enough to ensure ellipticity, but reading the calculation backwards, we see that only vectors of the form ${}^T(\frac{1}{\mu_1}, \frac{1}{\mu_2}, \ldots, \frac{1}{\mu_M}) f(t)$ cancel L.

To avoid this problem, we must find a way to fix this unknown function. We therefore define $\psi = \sum_{\alpha=1}^{M} \phi_\alpha$. We then compute $\sum_{\alpha=1}^{M} L(\phi)_\alpha$, finding :

$$r\Delta_x \psi = -\partial_t \bar{\rho} + \sum_{\alpha=1}^{M} \nabla.(r b_\alpha - m_\alpha) \ . \tag{43}$$

Summing up the boundary conditions in a periodic domain, we get :

$$\begin{cases} \bar{\rho}(0,.) - \sum_{\alpha=1}^{M} \rho_\alpha^0 = 0 \ , \\ \\ \bar{\rho}(T,.) - \sum_{\alpha=1}^{M} \rho_\alpha^T = 0 \ . \end{cases}$$

These conditions are always satisfied, since they refer to the compatibility of the constraints, wich we hope to be verified !

Remark 2.2. *If the domain is bounded, we have some other boundary conditions associated to (40) :*

$$\forall x \in \partial\Omega, \forall t \in [0;T], \ \partial_{\vec{n}} \phi_\alpha = (b_\alpha - \frac{m_\alpha}{r}).\vec{n} \ , \tag{44}$$

and to (43) :

$$\forall x \in \partial\Omega, \forall t \in [0;T], \ \partial_{\vec{n}} \psi = \sum_{\alpha=1}^{M} (b_\alpha - \frac{m_\alpha}{r}).\vec{n} \ . \tag{45}$$

In both bounded and periodic cases, we miss a boundary condition to fix the problem. This is not a surprise since the system was not of elliptic type, but we can observe that the indetermination deals uniquely with an additive function depending only on time. We can then decide to find ψ with a null mean for every t in $[0;T]$. Now we have an elliptic equation in ψ for every time.

Once we have ψ, ϕ is obtained solving the following laplace equation for every $\alpha \in [1;M]$:

$$
\begin{aligned}
r\mu_\alpha \Delta_{t,x}\phi_\alpha &= \frac{r}{\Gamma}\partial_{tt}\psi + \mu_\alpha \partial_t(ra_\alpha - \rho_\alpha) - \frac{1}{\Gamma}\partial_t\bar{\rho} \\
&\quad -\frac{1}{\Gamma}\sum_{\alpha'=1}^{M} \partial_t(ra_{\alpha'} - \rho_{\alpha'}) + \mu_\alpha \nabla.(rb_\alpha - m_\alpha)\ . \qquad (46)
\end{aligned}
$$

One can ask about the physical meaning of the arbitrary function. Looking at (38), we see that p is linked to ψ, and that adding such a function to ψ changes p just in such a way as to keep (27) valid. This is linked to the fact that only derivatives of ϕ are meaningful. We conclude this section by observing that fixing this unknown function is the way to restore injectivity of B.

2.4.2 Step B

We cannot differentiate L_r with respect to q. There is no coupling between the different phases for this step, so the minimization can be permormed phase by phase. q^n is then obtained by solving for every α :

$$
\begin{aligned}
\inf_{q_\alpha}[F_{\epsilon_1}(q_\alpha) \quad &+\tfrac{r}{2} < \nabla_{t,x}\phi_\alpha^n + \tilde{p}_\alpha^n - q_\alpha, \nabla_{t,x}\phi_\alpha^n + \tilde{p}_\alpha^n - q_\alpha > \\
&+ < l^n, \nabla_{t,x}\phi^n + \tilde{p}_\alpha^n - q >]\ ,
\end{aligned} \qquad (47)
$$

which is equivalent to :

$$
\inf_{q\in K} < q - \frac{r\nabla_{t,x}\phi^n + r\tilde{p}^n + l^n}{r+\epsilon_1}, q - \frac{r\nabla_{t,x}\phi^n + r\tilde{p}^n + l^n}{r+\epsilon_1} > .
$$

It is important to notice that this minimization can be performed pointwise in space and time. Let us set :

$$
P^n(t,x) = \{\alpha^n(t,x), \beta^n(t,x)\} = \frac{r\nabla_{t,x}\phi^n(t,x) + r\tilde{p}^n + l^n(t,x)}{r+\epsilon_1}.
$$

Then $q^n(t,x) = \{a^n(t,x), b^n(t,x)\}$ is obtained by solving :

$$
\begin{aligned}
&\inf \qquad [(a-\alpha^n(t,x))^2 + |b-\beta^n(t,x)|^2]. \\
\{a,b\}\ \ &s.t. a + \frac{|b|^2}{2} \le 0
\end{aligned}
$$

This is a simple one dimensional projection problem which can be computed analytically or using a Newton method.

2.4.3 Step C

Step C is simply the pointwise update :

$$
l^{n+1}(t,x) = l^n(t,x) + \delta^n(\nabla_{t,x}\phi^n(t,x) + \tilde{p}^n - q^n(t,x))\ .
$$

2.5 Cost and convergence criterium

Amongst these three steps, only Step A is global. This means that the cost of Step B and C are of order $O(N)$ where N is the number of points of the space-time lattice. The first Laplace equation (step A), due to the periodicity in space, can be solved in $O(N)$. The following Laplace equations (step A) can be solved in $O(NLog(N))$ operations. The cost of this methods is therefore of order $M \times Niter \times NLogN$ where $Niter$ is the necessary number of iteration n to converge and M the number of the phases.

We do not have theoretical estimates on the speed of convergence of the method. To be able to produce numerical estimates and also for the practical purpose of stopping the computation we need to define a convergence criterium. The optimality conditions (27) are useful for that purpose. We can indeed use the residual of the "vortex sheet equations" for each phase :

$$res_\alpha^n = \partial_t \phi_\alpha^n + \frac{|\nabla_x \phi_\alpha^n|^2}{2} + \frac{1}{\mu_\alpha} p^n \ ,$$

which is a by-product of the algorithm. This quantity converges to 0 as we approach the solution of problem. The normalized convergence criterium used is

$$crit^n = \frac{1}{M} \sum_{\alpha=1}^{M} \sqrt{\frac{\int_0^T \int_D \rho^n |res_\alpha^n|}{\int_0^T \int_D \rho^n |\nabla_x \phi_\alpha^n|^2}} \ . \tag{48}$$

3 1-dimensionnal numerical results

3.1 Numerical results obtained with Matlab

We present in this section numerical results obtained using a Matlab code. The algorithm first seems to converge, but after a hundred iterations, a bad behaviour appears, and the solution finally blows up. One can explain this by the fact that we used part of the Pde Matlab Toolbox, and therefore made many interpolations. In this case, the differential operators "div"and "grad" aren't still adjoint, and bad phenomena can occur.

3.1.1 Test 1

We compute the solutions in the box $[0;1]$ of problem (6,7,8,9) with two phases ; the initial and final densities are :

$$\begin{cases} \rho_1^0(x) = 0.4(1 + sin(\frac{\pi}{2}x)) + 0.1 \\ \rho_1^T(x) = 0.4(1 - sin(\frac{\pi}{2}x)) + 0.1 \\ \bar{\rho}(t,x) = 1 \end{cases} .$$

Figure 1 shows the two densities obtained after hundred iterations, when the convergence criterium is still very low, while figure 2 shows the convergence history. We see that after

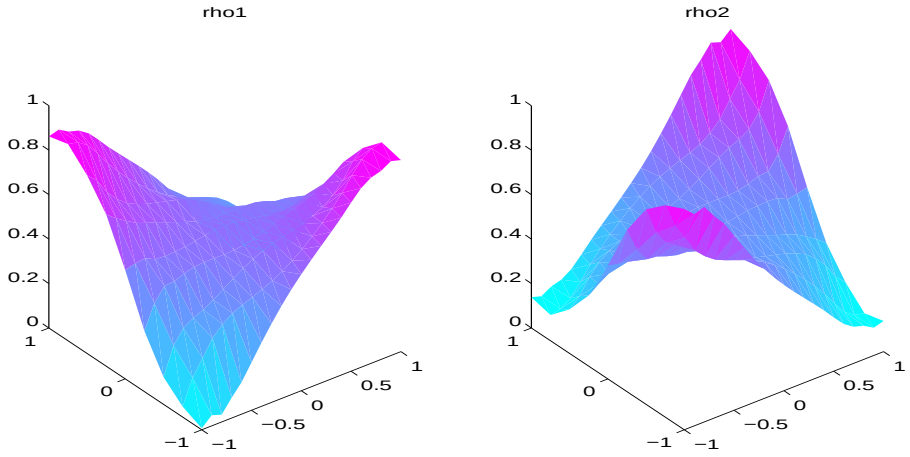

Figure 5: Densities after 100 iterations

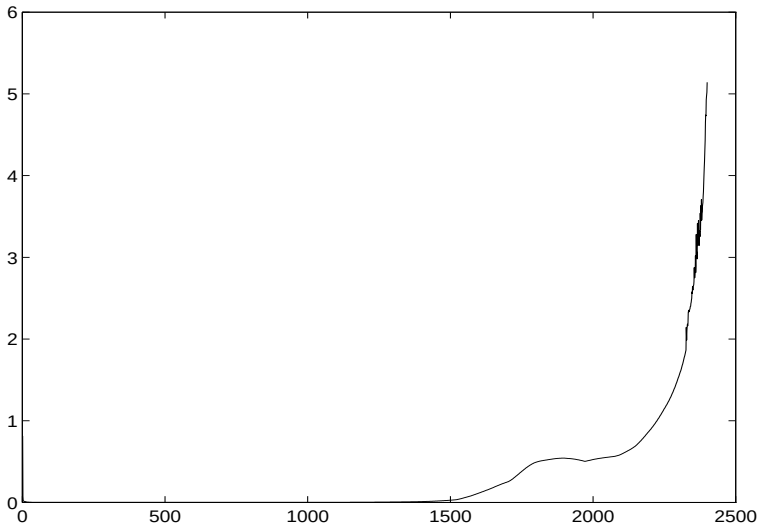

Figure 6: Convergence history

the first thousands iterations, the criterium begins to enlarge dramatically, expressing the fact that the densities are beginning to oscillate.

3.2 An alternative way to perform the computation

In [3], the concept of generalized flows for incompressible perfect fluids is introduced using a variationnal formulation between two prescripted states. An important class of those generalized flows consists in multiphasic flows. Since the fluid is incompressible, the sum of the densities in the different phases should be constant. We see then that we're not so far from our problem. Indeed, in the one-dimensionnal case, the order of the fluid particules in each phase is preserved, so that taking a final state adapted to the final density expected, we obtain the generalized flow minimizing (6). We can then use the lagrangian discretisation method introduced in [14] to compute solutions of problem (6,7,9,9)...

Roesch's algorithm constructs a sequel of permutation joining an initial state (taken to be the identity) to a final state represented by a permutation. It's then possible to follow each particle's trajectory. So all we have to do is to define the last permutation.

To do that, for each particle in the first state, we choose its phase so that the "discrete" densities are as close as possible to the precribed ones. We do exactly the same for the final state. Then having for each particle its phase number and its order in this phase, we choose the final permutation to respect those properties. Assuming the compatibility of the data, this shouldn't pose a problem. We then use Roesch's algorithm as its own to have the particle's trajectory. Since we want to compare the results with those obtained with the matlab code, we have to compute the densities. The discretization gives a density which weakly converges to the prescibed one. In order to evaluate Roesch's algorithm on this problem, we compute the relative error on the boundary. We then have following results :

$$\begin{cases} crit_1^m = \sqrt{\dfrac{\int_0^T \int_D \rho^m |res_\alpha^m|}{\int_0^T \int_D \rho^m |\nabla_x \phi_\alpha^m|^2}} = 1.241 \times 10^{-3} , \\ crit_2^r = \sqrt{\dfrac{\int_D (\rho_1^r(0,x) - \rho_1^0(x))^2 dx}{\int_D (\rho_1^0(x))^2 dx}} = 1.273 \times 10^{-2} , \\ error = \sqrt{\dfrac{\int_0^T \int_D (\rho_1^m(t,x) - \rho_1^r(t,x))^2 dx dt}{\int_0^T \int_D (\rho_1^m(t,x))^2 dx dt}} = 5.535 \times 10^{-2} . \end{cases}$$

We can think that the densities produced by Roesch's algorithm are everywhere in Q almost as close to the right solution as they are on the boundary. Thus we can estimate that the error computed comes mainly from our algorithm. It remains however quite small and we are not disappointed by it. In addition, we know about the oscillatory behavior of our solution, which is emphasized by the L^2 norm. But our convergence criterium seems not to be convenient in this case. Indeed, a closer look at the values of the lagrangian solution shows that on the boundary, it differs from the theoretic values in the same way as the particulate solution.

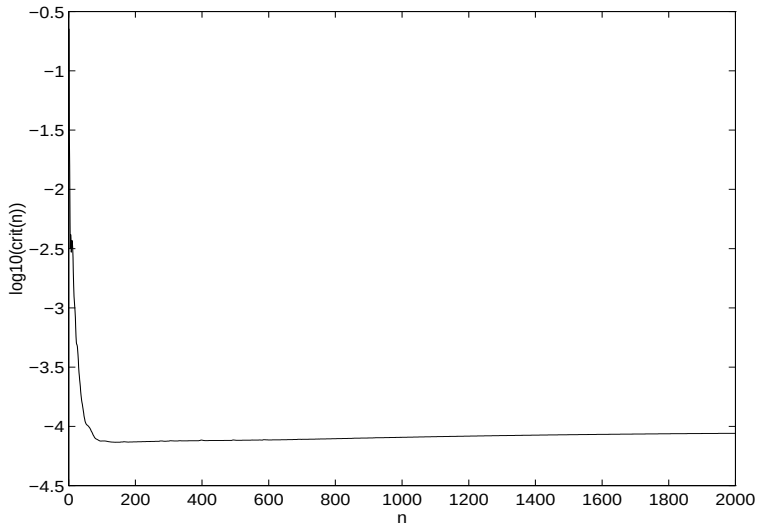

Figure 7: Convergence history

As we explained the bad behavior of the algorithm with the uncontrolled use of interpolations in the code, it's of great interest to see what happens when this problem is avoided. We can then use our periodic fortran 2D-code with 1D case-test. We have to say that in this code, the values on the boundary aren't weakly forced through a lagrange multiplier, but are imposed.

3.3 The 1-dimensionnal periodic case

In order to use Roesch's algorithm as its own, we have to find boundary data such that the periodic solution and the solution in the box coincide. Using symetric arguments, we see that it's the case for the following initial and final densities :

$$\begin{cases} \rho_1^0(x) = \chi_{[0;\frac{1}{4}]} + \chi_{[\frac{3}{4};1]} \ , \\ \rho_1^T(x) = \chi_{[\frac{1}{4};\frac{3}{4}]} \ , \\ \bar{\rho}(t,x) = 1 \ . \end{cases}$$

The convergence history for those data is given in Figure 7, while Figure 8 shows the results of both calculations : from the particulate method on the left, from our method after a hundred iterations on the right.

The convergence history shows that the criterium slowly grows up after a hundred iterations. We can explain that by the fact that we took $\epsilon_1 = 0$ and boundary data which

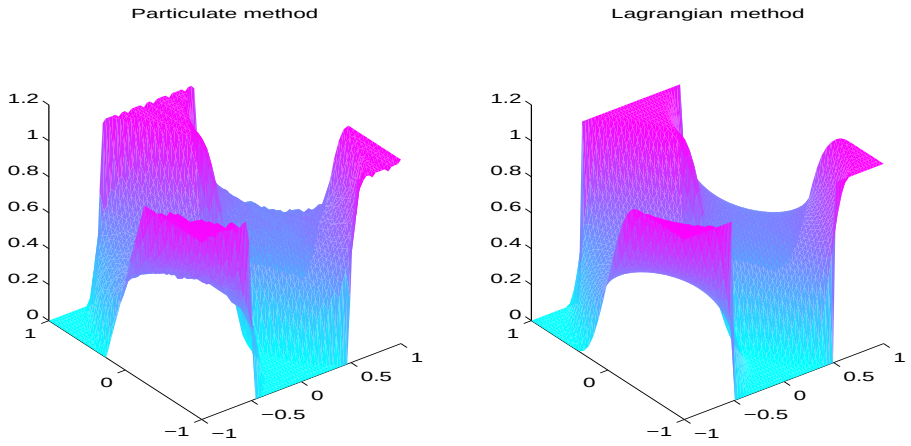

Figure 8: Densities after 100 iterations

vanishes. So we can't have the convergence property explained in section 2.6. The particulate method gives an unsmooth function, because the information given concerns the location of the particules and we have to go back to the densities with a counting method. We then lose precision in the reconstruction process. As in the previous subsection, we can compare the results :

$$\begin{cases} crit_1^l = \sqrt{\dfrac{\int_0^T \int_D \rho^l |res_\alpha^l|}{\int_0^T \int_D \rho^l |\nabla_x \phi_\alpha^l|^2}} = 7.53 \times 10^{-5} , \\ crit_2^r = \sqrt{\dfrac{\int_D (\rho_1^r(0,x) - \rho_1^0(x))^2 dx}{\int_D (\rho_1^0(x))^2 dx}} = 9.99 \times 10^{-2} , \\ error = \sqrt{\dfrac{\int_0^T \int_D (\rho_1^l(t,x) - \rho_1^r(t,x))^2 dx dt}{\int_0^T \int_D (\rho_1^l(t,x))^2 dx dt}} = 5.01 \times 10^{-2} . \end{cases}$$

In this case where the boundary data are discontinuous, they are badly approached by the particulate method, while the convergence criterium for the lagrangian method is very small. The difference between both methods is then of the same order as the particulate criterium. Thus we can suppose that our method gives good results.

4 2-dimensionnal numerical results

Our method seems to be able to compute generalized flows for which the number of phases is finite. In the framework of fluid mechanics, 1-dimensionnal tests are not of primary importance, and we are more interested in the study of 2-dimensionnal exemples. Moreover, following the approach of [6], ρ_α can be seen as a distance on the vertical axis. Then, our 2-dimensionnal model can be interpreted as a stratified 3-dimensionnal evolution model for height constrained inviscid flows.

4.1 First tests

We present in this section numerical tests. The normalized space-time domain is discretized using a regular $32 \times 32 \times 33$ lattice. Initial and final densities are represented, and are choosen to approach the ones used in [4]. It is then possible to see the qualitative difference between the monophasic and the multiphasic optimal mass transport problems. There we only present biphasic flows with equal weight coefficients for both phases ($\mu_1 = \mu_2$), and with a constant global density ($1 = \bar{\rho} = \rho_1 + \rho_2$). The densities in the first phase are all based on Gaussians densities or deformation of gaussians.

The parameters of the method are taken as $\epsilon_1 = 0$, $\epsilon_2 = 0.001$ and $r = 1$

Convergence history shows the convergence criterium (48) along the iterations of method ALG2. Convergence history even shows small erratic behavior after the first thousand iterations.

Finally, we give for different time steps the level curves of ρ. The final value of ρ at time step 33 always match ρ_T.

4.1.1 Test 1

In order to avoid the periodic effects, this test presents a small translation of a gaussian density. In such a case, the evolution of the density in the monophasic case is simply a translation with a constant velocity. We see here that the top of the gaussian do not translate with a constant velocity and that the gaussian is slightly diformed.

4.1.2 Test 2

We perform the translation and rotation of an elliptically deformed gaussian. Here we can easily see the transfer of a small amount of mass across the periodic boundaries. Again, we see that the velocity is not (mainly) constant.

4.1.3 Test 3

This test presents the largest possible translation (because of the periodic boundaries) for a gaussian density. As in the monophasic case, the gaussian splits into four parts. In contrast to the monophasic case where they were simply uniformly transfered on the edge of the torus, the points of biggest densities here seem to take a slower start, then to speed up, and

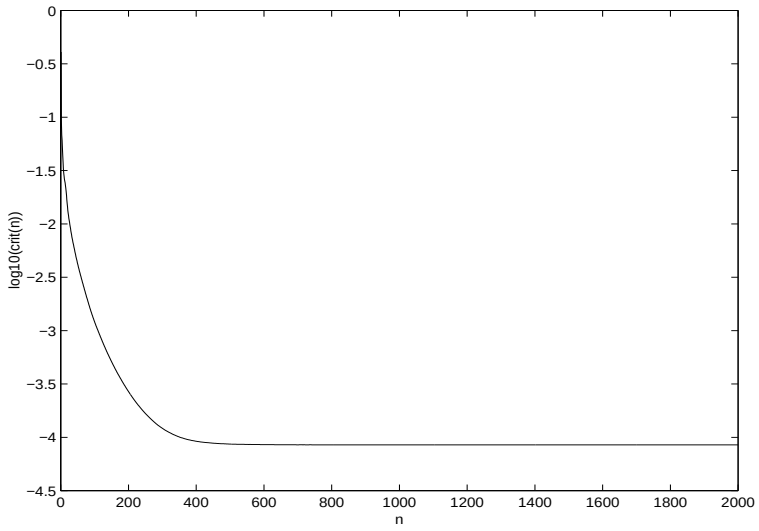

Figure 9: Convergence history

finally to slow down dramatically again. Maybe we can explain that by the fact that it's easier to travel when the other phase has almost the same "weight".

4.1.4 Test 4

In this test, we still take the translation of a gaussian density, but the total density is now varying with space and time. In the initial and final timesteps, we assume that the density of the second phase constant. The global density is then the linear interpolation in time of the extremal densities.

In the monophasic case, we could have use the following action :

$$K(\rho) = \int_D \int_0^T \partial_t \rho(t,x)^2 dx dt \, .$$

Then the solution of the time-continuous mass transport problem would be the linear interpolation of the initial and final densities. Therefore, we can see this this exemple as an interpolation between the L^2 and the Wasserstein minimization problems. Indeed, for fixed μ_1 and μ_2, if the "mass" of the second phase is taken equal to zero, we obtain the linear interpolation, while in the large, when this mass goes to infinity, the constraint on the first phase is negligeable, and in the limit, we recover the solution of the optimal mass transport problem.

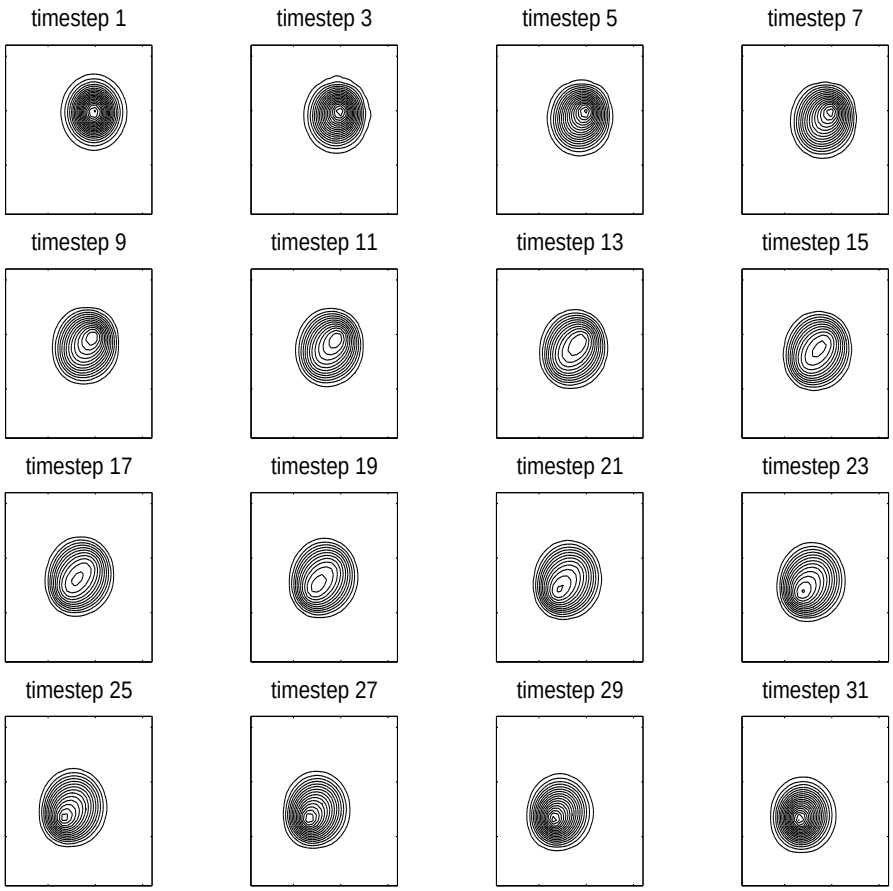

Figure 10: First density after 100 iterations

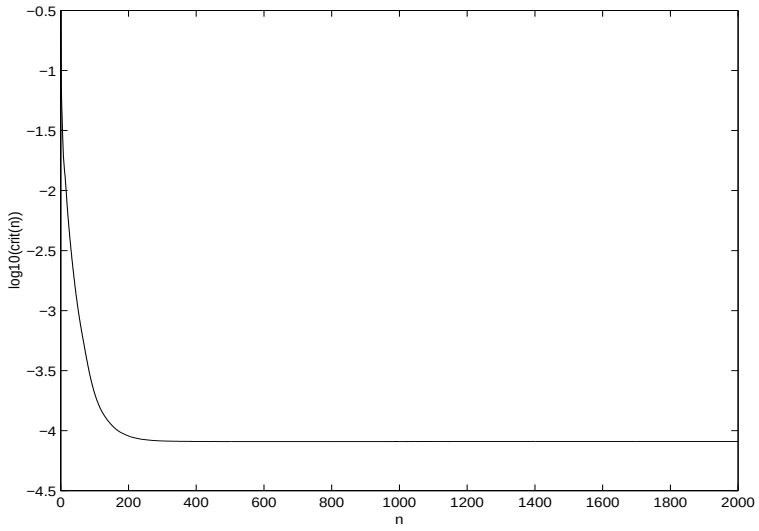

Figure 11: Convergence history

4.2 A possible validation of the method

In this section, our goal is to see if the kinetic energy is really minimized, and if the optimality equations are really computed. Those optimality conditions can be seen as evolution equations :

$$\begin{cases} \partial_t v_\alpha + (v.\nabla_x)v + \frac{1}{\mu_\alpha}\nabla_x p = 0 \ , \\ \partial_t \rho_\alpha + \nabla_x.(\rho_\alpha v_\alpha) = 0 \ , \\ v_\alpha(0,.) = \nabla_x \phi^0_\alpha(x) \ , \\ \rho_\alpha(0,.) = \rho^0_\alpha(.) \ . \end{cases} \tag{49}$$

Then a theoretical result allows us to construct some numerical examples :

Theorem 4.1. *Let $D = \mathbb{Z}^d/\mathbb{R}^d$.*
Let $(\rho^0_\alpha)_{\alpha=1,..,M} \in (C^\infty(D))^M$ and $(\phi^0_\alpha)_{\alpha=1,..,M} \in (C^\infty(D))^M$.
Let $p \in C^\infty([0;T] \times D)$ be a pressure field.
For every $\alpha \in \{1, ..., M\}$, we note (ρ_α, v_α) the solution of the evolution equations (49).

Then for a small time, (ρ_α, v_α) minimizes the kinetic energy (6) under constraints (7), (8) and (9).

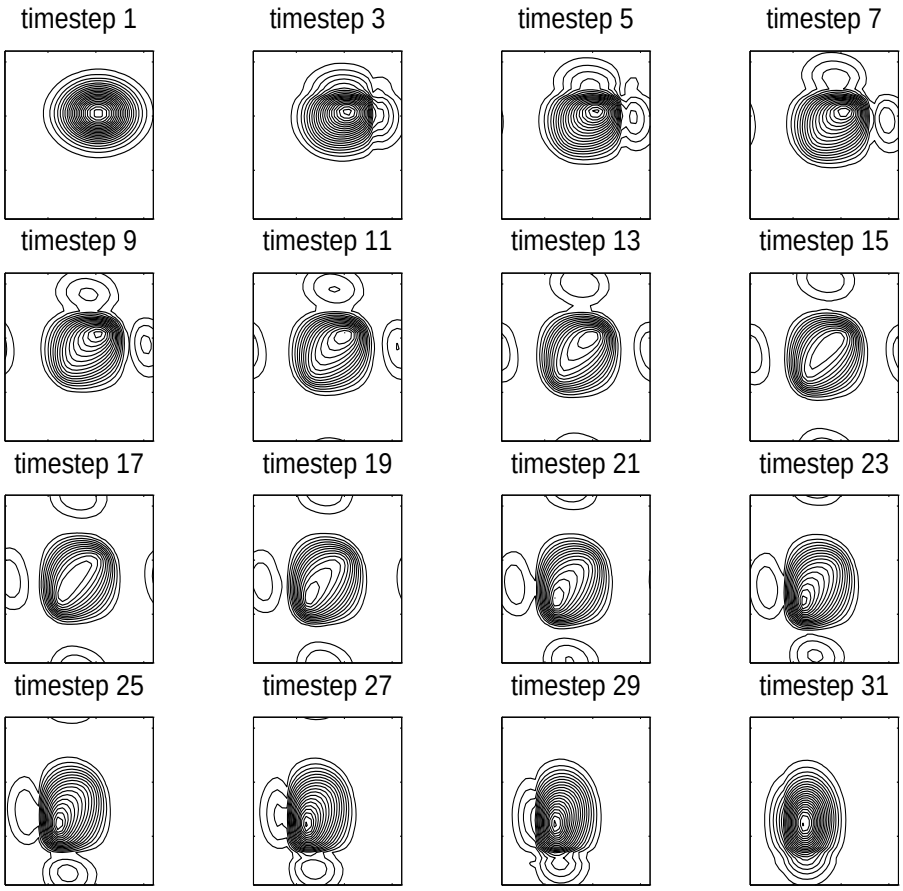

Figure 12: First density after 100 iterations

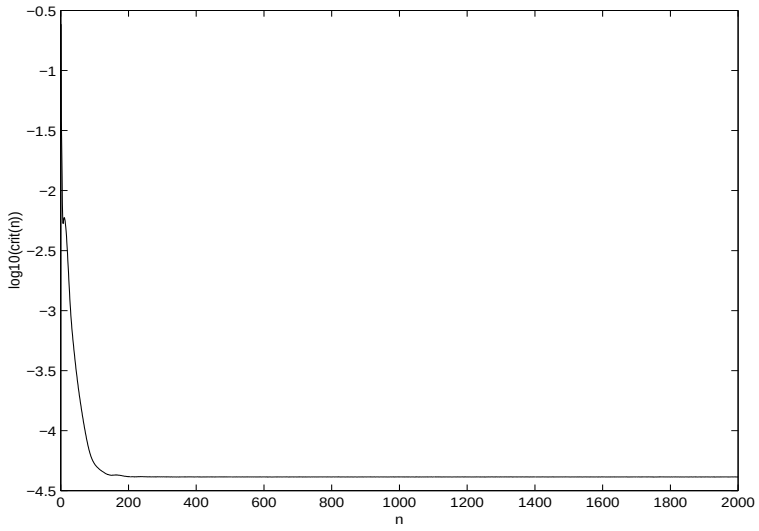

Figure 13: Convergence history

The proof of this theorem can be found in the first technical appendix. It mainly relies on the fact that for small times, the velocities remain potential.

4.3 Exemple 1

In this section, we take the pressure equal to zero. The pressure is the lagrange multiplier associated to the incompressibility constraint. Then we see that the phases would not "see" each other. It means that both phases would have a "monophasic-style" evolution. Indeed, in such a case, the characteristics are just straight lines, just as in the monophasic case. Therefore, our results should match the monophasic results for each phase.

For the initial functions ϕ_α^0, we take :

$$\begin{cases} \phi_1^0 = \dfrac{1}{8\pi^2}(\sin(2\pi x) + \cos(2\pi y)) \ , \\ \\ \phi_2^0 = 0 \ . \end{cases} \tag{50}$$

The initial densities are both taken to be 1, and from the pressure and the initial velocity field in the second phase, we see that the density is always equal to 1 in the second phase. For those initial data (expressed in the appendix), the time condition simplifies. Here, we should have $\|D_{xx}\phi_1^0\| \ T < 1$. But the norm of $D_{xx}\phi_1^0$ is easily shown to be $4\pi^2$. We can therefore take $T = 1$.

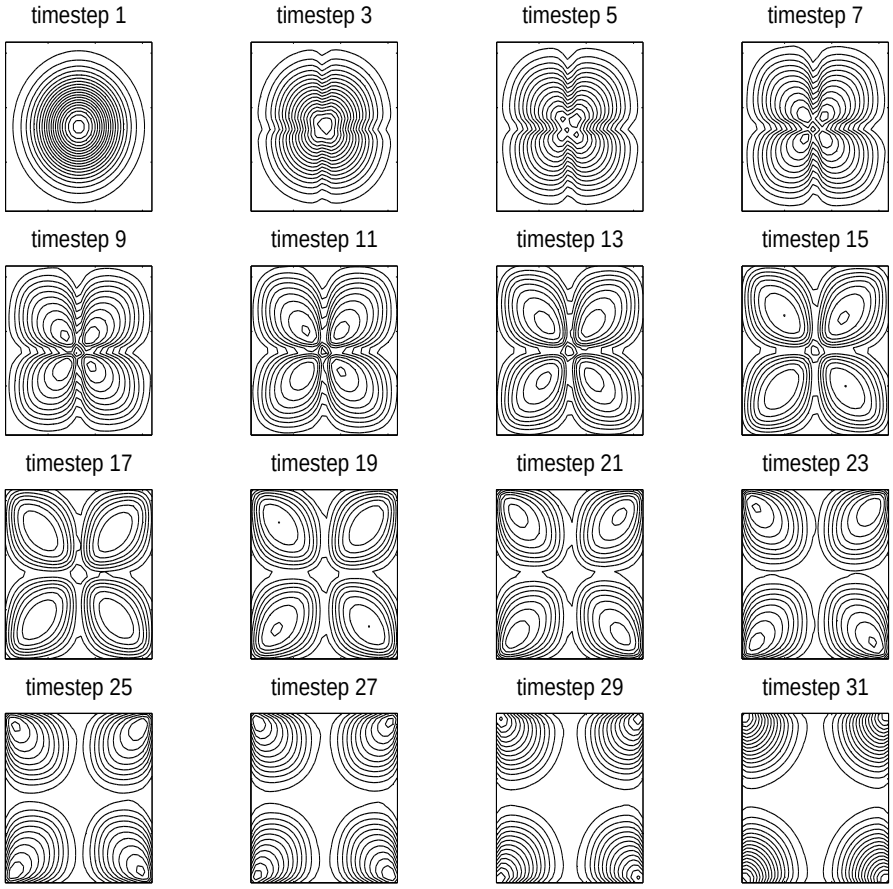

Figure 14: First density after 100 iterations

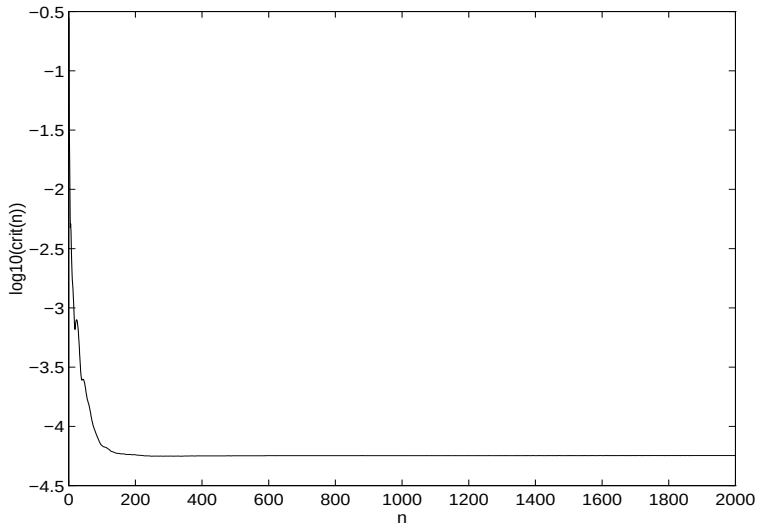

Figure 15: Convergence history

The theoretical density in the first phase can easily be computed using a newton method. Once the theoretical densities in both phases are known, we can use the global density and the final and initial densities as entries for our algorithm. We can then see the L^2 norm of the pressure and the relative L^2 norm of the density in the second phase. The computations are made on a regular $32 \times 32 \times 33$ latice. After one hundred iterations, we find :

$$\begin{cases} \|p\|_{L^2(Q)} = 2.66 \times 10^{-4} \ , \\ \\ \|\rho_2 - \bar{1}\|_{L^2(Q)} = 2.32 \times 10^{-3} \ . \end{cases}$$

We can also see the convergence history on Figure 17 and the evolution of the density in the first phase on Figure 18.

4.4 Example 2

Now we solve numerically the equations, and then compute the densities. The initial densities are both choosen equal to 1.

In this test, we take the following pressure :

$$p(t,x,y) = \frac{t}{8\pi} \cos(2\pi x) \ . \tag{51}$$

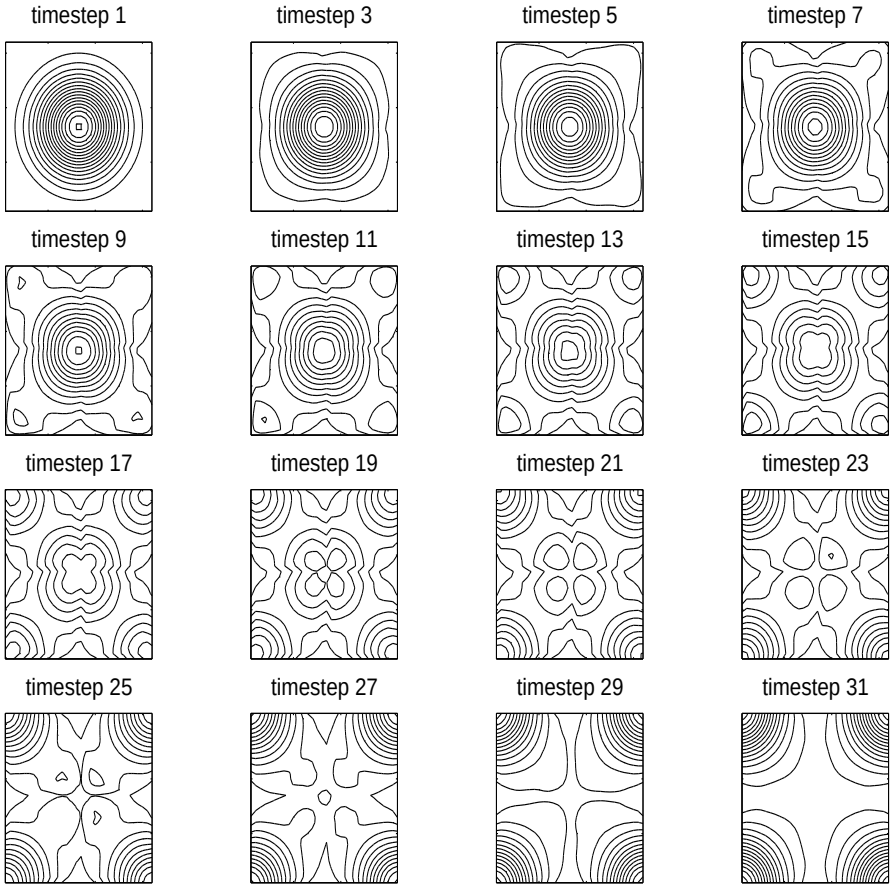

Figure 16: First density after 100 iterations

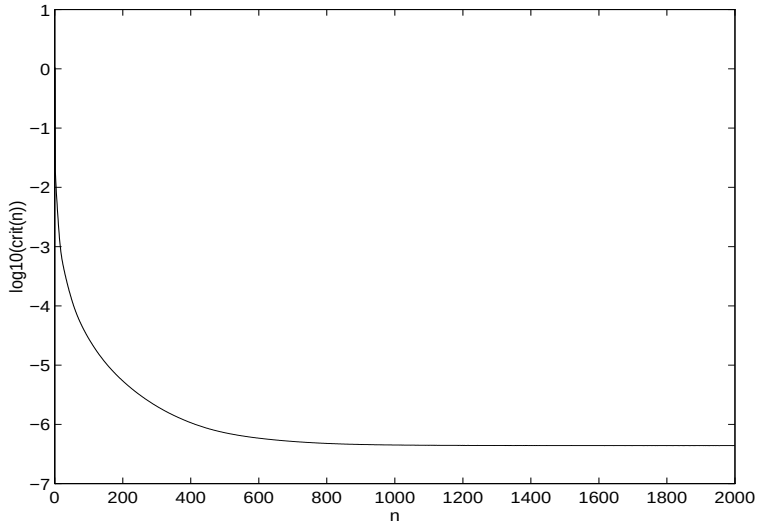

Figure 17: Convergence history

The initial functions ϕ_α^0 are :

$$\begin{cases} \phi_1^0(x,y) = \dfrac{1}{8\pi^2}\sin(2\pi y)\ , \\ \\ \phi_2^0(x,y) = 0\ . \end{cases} \tag{52}$$

With those values, we compute that condition (56) is satisfied if $T < 0.62$. But the particles don't cross at this time, and we can still take $T = 1$.

The densities and the pressure are still well computed :

$$\begin{cases} \dfrac{\|\rho_1^l - \rho_1^{ref}\|_{L^2(Q)}}{\|\rho_1^{ref}\|_{L^2(Q)}} = 1.49 \times 10^{-3}\ , \\ \\ \dfrac{\|\rho_2^l - \rho_2^{ref}\|_{L^2(Q)}}{\|\rho_2^{ref}\|_{L^2(Q)}} = 1.53 \times 10^{-3}\ , \\ \\ \dfrac{\|p^l - p^{ref}\|_{L^2(Q)}}{\|p^{ref}\|_{L^2(Q)}} = 1.70 \times 10^{-2}\ . \end{cases}$$

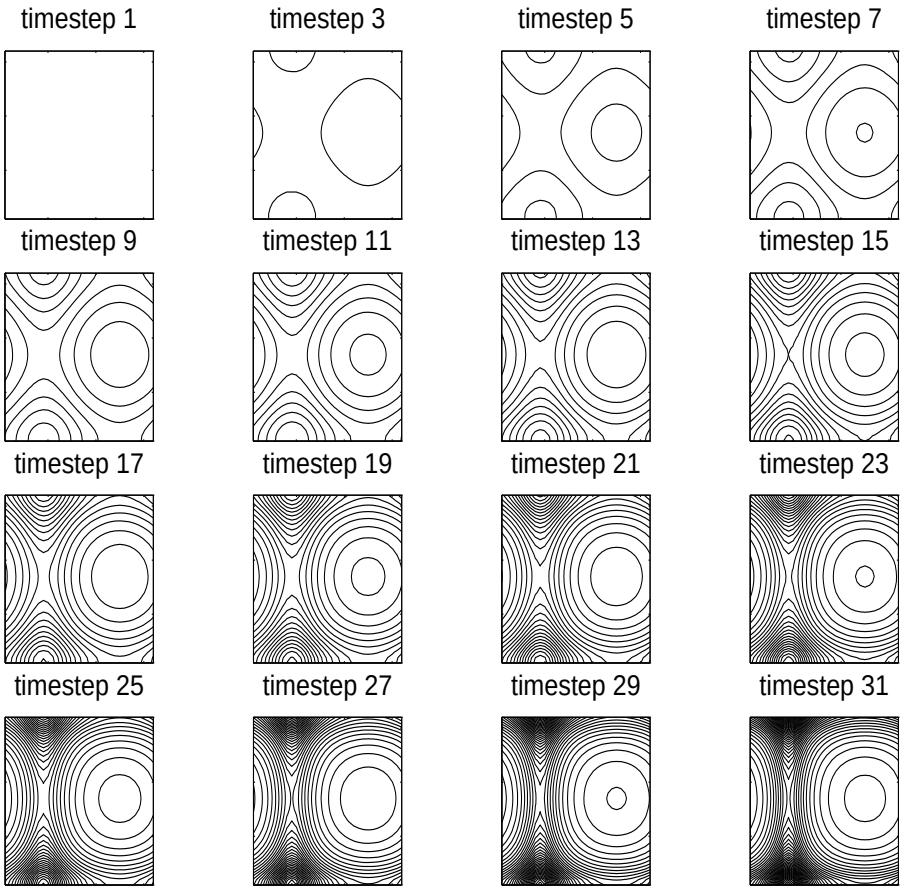

Figure 18: First density after 100 iterations

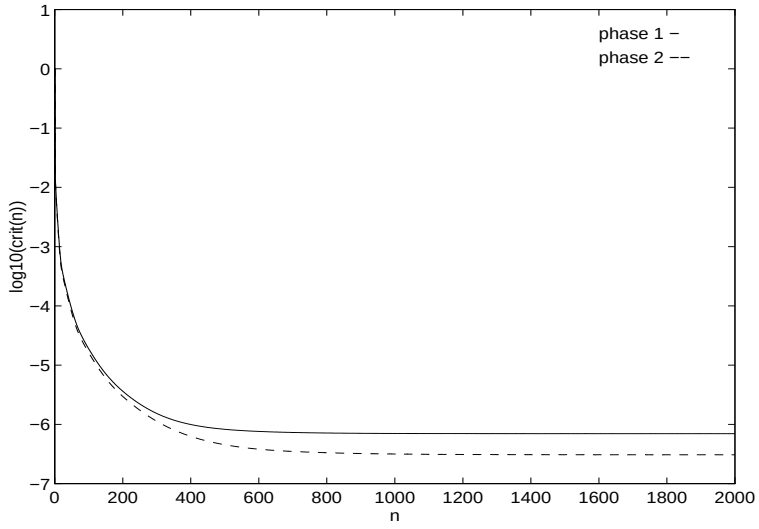

Figure 19: Convergence history

The convergence history for both phases is shown on figure 19, while the evolution of the first density can be seen on figure 20.

4.5 Example 3

As in the previous section, we use here a finite difference sheme to solve system (57). This example is a little more complicated, but still shows good convergence properties. In this test, the pressure depends on both space directions, and is taken as follows :

$$p(t,x,y) = \frac{1}{4\pi^2}\cos(2\pi x)\sin(2\pi y + \frac{\pi}{6}) \ . \tag{53}$$

The initial functions ϕ_α^0 are :

$$\begin{cases} \phi_1^0(x,y) = \dfrac{1}{16\pi^2}\sin(2\pi y) \ , \\ \\ \phi_2^0(x,y) = \dfrac{1}{8\pi^2}\cos(2\pi x) \ . \end{cases} \tag{54}$$

Just as in the previous exemple, we have a good recovery of the densities. The results for the pressure aren't that good, due to the fact that we take the relative error, and that the pressure is very small. Therefore, a little L^2-norm error can turn into a significant relative

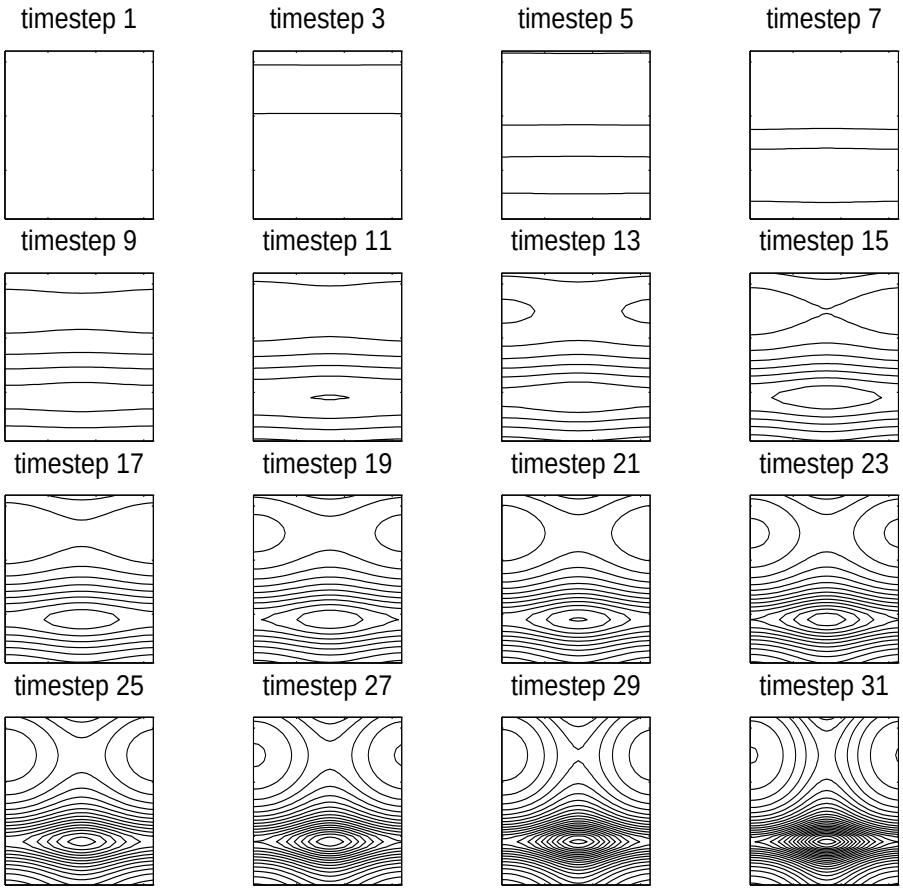

Figure 20: First density after 100 iterations

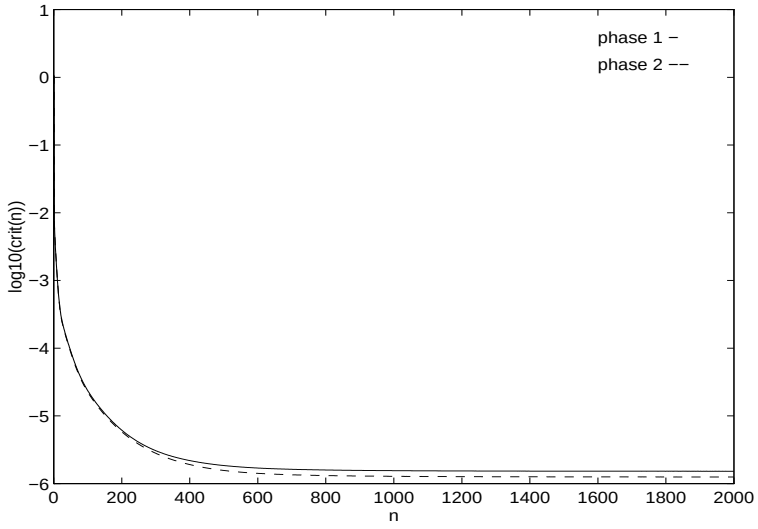

Figure 21: Convergence history

error. Moreover, the pressure was first used to compute the densities. Since the limit time is taken very close to the time when the characteristics cross, the densities begin to have a huge L^∞-norm. Therefore, the error in the first step of our computation, the evaluation of the global density, can be quite big. The densities, however, aren't so dependent on this first approximation, since the global density is taken as data, while the pressure is forgotten.

The convergence history is shown on figure (21), while figure (22) attemps to show the evolution of the whole fluid.

$$\begin{cases} \dfrac{\|\rho_1^l - \rho_1^{ref}\|_{L^2(Q)}}{\|\rho_1^{ref}\|_{L^2(Q)}} = 3.25 \times 10^{-2} \ , \\ \dfrac{\|\rho_2^l - \rho_2^{ref}\|_{L^2(Q)}}{\|\rho_2^{ref}\|_{L^2(Q)}} = 3.28 \times 10^{-2} \ . \\ \dfrac{\|p^l - p^{ref}\|_{L^2(Q)}}{\|p^{ref}\|_{L^2(Q)}} = 0.11 \ . \end{cases}$$

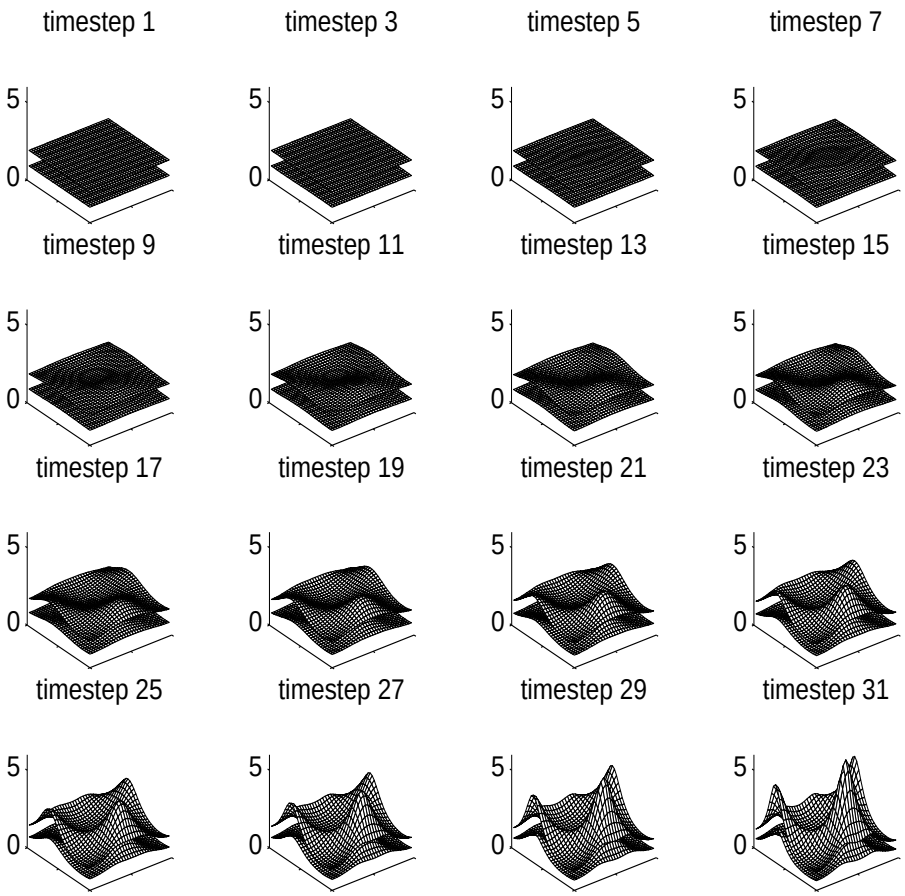

Figure 22: First density after 100 iterations

Appendix A : Proof of theorem 4.1

In this appendix, a proof of theorem 4.1 is given. We remind the content of the theorem :

Theorem 4.2. *Let $D = \mathbb{Z}^d/\mathbb{R}^d$.*
Let be $(\rho_\alpha^0)_{\alpha=1,..,M} \in (C^\infty(D))^M$ and $(\phi_\alpha^0)_{\alpha=1,..,M} \in (C^\infty(D))^M$.
Let $p \in C^\infty([0;T] \times D)$ be a pressure field.
For every $\alpha \in \{1, ..., M\}$, we note (ρ_α, v_α) the solution of :

$$\begin{cases} \partial_t v_\alpha + (v.\nabla_x)v + \frac{1}{\mu_\alpha}\nabla_x p = 0 \ , \\ \partial_t \rho_\alpha + \nabla_x.(\rho_\alpha v_\alpha) = 0 \ , \\ v_\alpha(0,.) = \nabla_x \phi_\alpha^0(x) \ , \\ \rho_\alpha(0,.) = \rho_\alpha^0(.) \ . \end{cases} \tag{55}$$

Let $T > 0$ and note λ the largest eigenvalue of $D_{xx}p$ in $[0;T] \times D$.

Then under the condition that :

$$\sup_{\alpha \in \{1,...,M\}} (\|D_{xx}\phi_\alpha^0\| T + \lambda \frac{T^2}{2\mu_\alpha}\sqrt{d}) e^{\lambda \frac{T^2}{2}} < 1 \ , \tag{56}$$

the solution of system (55) minimizes the kinetic energy :

$$K(\rho, v) = \sum_{\alpha=1}^{M} \mu_\alpha \int_0^T \int_D \rho_\alpha(t,x)|v_\alpha(t,x)|^2 dxdt \ .$$

under constraints (7), (8) and (9).

Remark 4.3. *Condition (56) is very restrictive. It's sufficient to know that at each $t < T$, the map $X_\alpha(t,.)$ is a diffeomorphism on the torus. In our numerical experiments, this is always the case when the densities stay bounded. Therefore, we wouldn't always respect condition (56) in our applications.*

Proof. First, we define the characteristics X_α of system (55). These characteristics are solutions of the following system :

$$\begin{cases} d_{tt}X_\alpha(t,x) = -\frac{1}{\mu_\alpha}\nabla_x p(t, X_\alpha(t,x)) & \text{in } [0;T] \times D \ , \\ d_t X_\alpha(0,x) = \nabla_x \phi_\alpha^0(x) & \text{in } D \ , \\ X_\alpha(0,x) = x & \text{in } D \ . \end{cases} \tag{57}$$

Under our regularity assumptions on the data, which are much stronger than really needed, we can apply the Cauchy-Lipschitz theorem, finding that for each x in D, the differential equation (57) has a unique solution on $[0;T]$. Moreover, this solution is in $C^\infty([0;T]\times D)$.

Next, we show that for every fixed t in $[0;T]$, $X_\alpha(t,.)$ is a diffeomorphism from D to D. For every couple (t,x) in $[0;T]\times D$, we note :

$$\begin{cases} y_\alpha(t,x) = D_x X_\alpha(t,x) \ , \\ \tilde{M}_\alpha(t,x) = -\frac{1}{\mu_\alpha}[D_{xx}p](t,X_\alpha(t,x)) \ . \end{cases}$$

We have then :

$$\begin{cases} \ddot{y}_\alpha(t,x) = \tilde{M}_\alpha(t,x) y_\alpha(t,x) \ , \\ \dot{y}_\alpha(0,x) = D_{xx}\phi^0_\alpha(x) \ , \\ y_\alpha(0,x) = Id \ . \end{cases}$$

Using taylor's formula, we get :

$$y_\alpha(t,x) - y_\alpha(0,x) = t\ D_{xx}\phi^0_\alpha + \int_0^t (t-u)\tilde{M}_\alpha(u,x) y_\alpha(u,x) du \ .$$

Let $\Psi(t,x) = \|y_\alpha(t,x) - y_\alpha(0,x)\|$. We have :

$$\begin{aligned} \Psi(t,x) &\leq t\ \|D_{xx}\phi^0_\alpha\| + \lambda \textstyle\int_0^t (t-u)\Psi(t,u)du + \lambda \int_0^t (t-u)\|y_\alpha(0,x)\| \ , \\ &\leq t\ \|D_{xx}\phi^0_\alpha\| + \lambda\tfrac{t^2}{2}\|y_\alpha(0,x)\| + \lambda \textstyle\int_0^t (t-u)\Psi(t,x)du \ , \\ &\leq t\ \|D_{xx}\phi^0_\alpha\| + \lambda\tfrac{t^2}{2}\sqrt{d} + \lambda \textstyle\int_0^t (t-u)\Psi(t,x)du \ , \end{aligned}$$

Applying Gronwall's Lemma, we get :

$$\Psi(t,x) \leq (\|D_{xx}\phi^0_\alpha\|\ t + \lambda\frac{t^2}{2}\sqrt{d})e^{\lambda\frac{t^2}{2}} < 1$$

The function "determinant" is continuous on the square matrix. Better, we know yet that if $\|M\| < 1$, then $\det(I+M) > 0$. Therefore, we deduce from the last formula that for every (t,x) in $[0;T]\times D$, we have $\det(y_\alpha(t,x)) > 0$.

Looking at the function $X_\alpha(t,.)$ as a function from $\mathbb{R}^d$ to $\mathbb{R}^d$, we obtain : $X_\alpha(t,x+n) = X_\alpha(t,x) + n$ for every n in $\mathbb{Z}^d$. Moreover, $X_\alpha(t,.)$ is of the class C^1, proper, and satisfies $\det(D_x X_\alpha(t,x)) > 0$ for every (t,x) in $\mathbb{R}^d$. We apply Hadamard's Lemma, obtaining that X_α is a global C^1 diffeomorphism. Thus we deduce that v is defined on the whole torus.

For the sake of simplicity, we only look at the 2-dimensionnal case (the arguments are identical in higher dimensions). The curl is transported by the flow, satisfying :

$$\partial_t \omega_\alpha + (v_\alpha . \nabla_x)\omega_\alpha - \omega_\alpha \nabla_x . v_\alpha = 0 \ . \tag{58}$$

So, we have :

$$\begin{cases} d_t \omega(t, X_\alpha(t,x)) - \omega(t, X_\alpha(t,x)) \nabla_x . v_\alpha(t, X_\alpha(t,x)) = 0 & \text{in } [0;T] \times D \ , \\ \omega(0,x) = 0 & \text{in } D \ . \end{cases} \tag{59}$$

Applying the Cauchy-Lipschitz theorem for system (59), we obtain the existence and unicity of a solution on $[0;T]$ for every x in D. But 0 is a solution. So the curl is everywhere zero in $[0;T] \times D$. Therefore, the velocity field is potential, that is :

$$\exists \phi_\alpha, \forall (t,x) \in [0;T] \times D, v_\alpha(t,x) = \nabla_x \phi_\alpha(t,x) \ . \tag{60}$$

Moreover, simple calculation shows that those functions satisfy :

$$\begin{cases} \partial_t \phi_\alpha + \frac{1}{2} |\nabla_x \phi_\alpha|^2 + \frac{1}{\mu_\alpha} p = 0 & \text{in } [0;T] \times D \ , \\ \phi_\alpha(0,.) = \phi_\alpha^0(.) & \text{in } D \ . \end{cases} \tag{61}$$

Let $(\tilde{\rho}_\alpha, \tilde{v}_\alpha)_{\alpha=1,..,M}$ be some functions satisfying (8) and (9). The characterstic curves are denoted respectively by $g_\alpha(.,.)$ and $\tilde{g}_\alpha(.,.)$. We have :

$$\begin{aligned} &\int_Q [\rho_\alpha(t,x)\partial_t \phi_\alpha + \rho_\alpha(t,x)|\nabla_x \phi_\alpha|^2] dx dt \\ &= \int_Q [\tilde{\rho}_\alpha(t,x)\partial_t \phi_\alpha + \tilde{\rho}_\alpha(t,x).\tilde{v}_\alpha(t,x)\nabla_x \phi_\alpha] dx dt \\ &= \int_Q \rho_\alpha^0(x)[\partial_t \phi_\alpha(t, \tilde{g}_\alpha(t,x)) + \partial_t \tilde{g}_\alpha(t,x).\nabla_x \phi_\alpha(t, \tilde{g}_\alpha(t,x))] dx dt \end{aligned}$$

$$= \int_Q \rho_\alpha^0(x)\{\ [\partial_t\phi_\alpha + \frac{1}{2}|\nabla_x\phi_\alpha|^2 + \frac{p}{\mu_\alpha}](t,\tilde{g}_\alpha(t,x))$$
$$-\frac{1}{2}|\partial_t\tilde{g}_\alpha(t,x) - \nabla_x\phi_\alpha(t,\tilde{g}_\alpha(t,x))|^2 + |\partial_t\tilde{g}_\alpha(t,x)|^2$$
$$-\frac{p}{\mu_\alpha}(t,\tilde{g}_\alpha(t,x))\ \}dxdt\ .$$

Let $E_\alpha(\rho_\alpha, v_\alpha) = \int_Q \rho_\alpha(t,x)\|v_\alpha(t,x)\|^2 dxdt$. We have :

$$\tilde{E}_\alpha + \int_Q \rho_\alpha^0(x)\{\ [\partial_t\phi_\alpha + \frac{1}{2}|\nabla_x\phi_\alpha|^2 + \frac{p}{\mu_\alpha}](t,\tilde{g}_\alpha(t,x))$$
$$-\frac{1}{2}|\partial_t\tilde{g}_\alpha(t,x) - \nabla\phi_\alpha(t,\tilde{g}_\alpha(t,x))|^2\ \}dxdt$$
$$= \int_Q \rho_\alpha(t,x)[\partial_t\phi_\alpha + |\nabla_x\phi_\alpha|^2 + \frac{p}{\mu_\alpha}]dxdt$$
$$+\int_Q \rho_\alpha^0(x)[\frac{p}{\mu_\alpha}(t,\tilde{g}_\alpha(t,x)) - \frac{p}{\mu_\alpha}(t,g_\alpha(t,x))]dxdt$$
$$= E_\alpha + \int_Q \rho_\alpha(t,x)[\partial_t\phi_\alpha + \frac{1}{2}|\nabla_x\phi_\alpha|^2 + \frac{p}{\mu_\alpha}](t,x)dxdt$$
$$+\int_Q \frac{p}{\mu_\alpha}(t,x)[\tilde{\rho}_\alpha - \rho_\alpha](t,x)dxdt\ .$$

Noting that $\sum_{\alpha=1}^M \rho_\alpha \equiv \bar{\rho} \equiv \sum_{\alpha=1}^M \tilde{\rho}_\alpha$ and summing up in α the previous equation, we obtain :

$$\sum_{\alpha=1}^M \mu_\alpha E_\alpha = \sum_{\alpha=1}^M \mu_\alpha \tilde{E}_\alpha - \frac{1}{2}\sum_{\alpha=1}^M \mu_\alpha$$
$$\int_Q \rho_\alpha^0(x)|\partial_t\tilde{g}_\alpha(t,x) - \nabla_x\phi_\alpha(t,\tilde{g}_\alpha(t,x))|^2 dxdt\ .$$

And then :

$$\sum_{\alpha=1}^M \mu_\alpha E_\alpha \leq \sum_{\alpha=1}^M \mu_\alpha \tilde{E}_\alpha\ .$$

This completes the proof of theorem 4.1.

Appendix B : On practical facilities with the algorithm

A highly interesting issue would be to prove a global convergence result for the numerical scheme as the discretization parameters go to zero. This seems to be difficult, since ALG2 has to be used in a hilbertian frame work, which is not the case in the infinite dimensionnal problem. In the discrete problem anyway, we can prove the convergence of the algorithm to a saddle point of the problem. This is done in [23] under uniform convexity assumptions. As mentioned previously, we observe in practice that the discrete algorithm converges even when ϵ_1 is taken null. We give here a proof for this phenomenon, which is closely related to the classical convergence proof for ALG2 given in [23].

Theorem 4.4. *Assume that the following holds.*
(i) The lagrangian L_r as a saddle-point $\{\phi, p, q, l\}$.
(ii) There exists $\lambda > 0$ such that for each α, $l_\alpha = (\rho_\alpha, m_\alpha)$ satisfies

$$\forall (t,x) \in Q, \rho_\alpha(t,x) \geq \lambda \, .$$

Then, if δ^n satisfies

$$0 < \delta^n = \delta < \frac{1+\sqrt{5}}{2} \, r, \tag{62}$$

the sequence ϕ^n, p^n, q^n, l^n computed in ALG2 is well defined and satisfies

$$\begin{cases} F(q^n) + G(\phi^n, p^n) \to F(q) + G(\phi, p) \, , \\ \phi^n, p^n, q^n, l^n \to \phi, p, q, l^* \, , \end{cases}$$

$\{\phi, p, q, l^*\}$ being a saddle-point of L_r. Moreover, depending on the discretization of the problem, we can have $l^* = l$.

Proof. Following the proof of Theorem 4.2 in [23], we get :

$$\begin{cases} |l^n|, |q^n|, |B(\phi^n, p^n)| \text{ are bounded} \, , \\ \lim\limits_{n\to\infty} |B(\phi^n, p^n) - q^n| = \lim\limits_{n\to\infty} |p^n - p^{n-1}| = 0 \, , \\ \lim\limits_{n\to\infty} (F(q^n) + G(\phi^n)) = F(q) + G(\phi) \, , \\ G(\phi^n) + (l, B(\phi^n, p^n)) \geq G(\phi) + (l, B(\phi, p)) \, , \\ F(q^n) - (l, q^n) \geq F(q) - (l, q) \, . \end{cases} \tag{63}$$

Since $F_{|K} \equiv 0$, we have that :

$$\forall n \in N, (l, q) \geq (l, q^n)$$

We also have that $G(\phi^n)$ converges to $G(\phi)$ when n goes to infinity. We have then $(l, B(\phi^n, p^n) - B(\phi, p)) \geq G(\phi) - G(\phi^n)$. Considering the fact that $|B(\phi^n, p^n) - q^n| \to 0$, we get :

$$\liminf_{n\to\infty}(l, q^n - q) \geq 0$$

We then have $(l, q^n - q)$ converges to zero when n goes to infinity. Since the problem is discrete, we just have to prove that for every point $(l, q^n - q)$ converges to zero impluing that q^n converges to q. We use the following proposition :

Lemma 4.5. *Let K be a closed convex set in R^d and a,l two vectors such that :*

$$\begin{cases} a \in K \\ \\ \forall x \in K \backslash \{a\},\ (l, x) > (l, a). \end{cases}$$

Let $(u_n)_{n\in N}$ be a bounded sequence in K^N such that $\lim_{n\to\infty}(l, u_n) = (l, a)$, then u_n converges to a as n goes to infinity.

Taking q for a and applying the proposition, we get :

$$\lim_{n\to\infty} |q^n - q| = 0.$$

We then get from (63) the convergence of $B(\phi^n, p^n)$ towards $B(\phi, p)$ and hence the convergence of (ϕ^n, p^n) towards (ϕ, p) because B is injective and continuous (and therefore has a closed range).

We have that $|l^n|$ is bounded, so we can extract a subsequence converging to l^*, which is easily seen to satisfy that $\{\phi, p, q, l^*\}$ is a saddle-point of L_r.

Easy calculations using the definition of a saddle-point show that :

$$q_\alpha = (\frac{|m_\alpha|^2}{2\rho_\alpha^2}, \frac{m_\alpha}{\rho_\alpha}) = (\frac{|m_\alpha^*|^2}{2\rho_\alpha^{*2}}, \frac{m_\alpha^*}{\rho_\alpha^*})\ . \tag{64}$$

Notating $q_\alpha = (a_\alpha, b_\alpha)$, we see that both ρ_α and ρ_α^* are formally solution of the problem :

$$\begin{cases} \partial_t \rho_\alpha + \nabla.(\rho_\alpha b_\alpha) = 0 \\ \rho_\alpha(0, .) = \rho_\alpha^0\ . \end{cases} \tag{65}$$

Indeed, the discrete analogous of (65) holds. The resulting system depends on the discretization method. In our case, we used a finite differences scheme, and letting n tend to infinity, injecting the pointwise equalities in Step C and in equation (64) in system (40), (41), we get :

$$\begin{cases} \dfrac{\rho_{\alpha,i,j}^{k+1} - \rho_{\alpha,i,j}^{k}}{\delta t} + \dfrac{(b_\alpha \rho_\alpha)_{i,j}^{k+1} - (b_\alpha \rho_\alpha)_{i-1,j}^{k+1}}{\delta x} + \dfrac{(b_\alpha \rho_\alpha)_{i,j}^{k+1} - (b_\alpha \rho_\alpha)_{i,j-1}^{k+1}}{\delta y} = 0 \ , \\ \rho_{\alpha,i,j}^{1} = \rho_\alpha^0(x_i, y_j) \ , \\ \rho_{\alpha,i,j}^{n_T} = \rho_\alpha^T(x_i, y_j) \ . \end{cases} \tag{66}$$

Once we know b_α, this system has only one solution. We deduce then that $l_\alpha^* = l_\alpha$ is the only possible limit for l_α^n. It follows that all the sequence converges to l^α. This completes the proof of theorem 4.4.

Appendix C : From the biphasic to the monophasic case

In order to perform one more validation of the method, we can study the limiting case in two phases, when one parameter goes to zero. This limit was often used during the programmation, because it allowed a comparison with the monophasic code, which was known to work. In this case, we expect that constraint (8) becomes :

$$\rho_1 \leq \bar{\rho} \ . \tag{67}$$

In the case when the monophasic optimal map for the first phase is always smaller than $\bar{\rho}$, we expect a recovery of the monophasic results. This is confirmed by the following theorem :

Theorem 4.6. *Let $(\rho_1^{opt}, v_1^{opt})$ the monophasic optimal couple from ρ_1^0 to ρ_1^T. We define L_r :*

$$\begin{aligned} L_r(\rho, v) &= \int_0^T \int_D \rho_1(t,x) |v_1(t,x)|^2 dx dt \\ &\quad + r \int_0^T \int_D \rho_2(t,x) |v_2(t,x)|^2 dx dt \ . \end{aligned} \tag{68}$$

Let (ρ_1^r, v_1^r) the biphasic optimal couple for L_r. Suppose that there exists $\beta > 0$ such that :

$$\begin{cases} \forall (t,x) \in [0;T] \times D, \ \beta \leq \rho_1^{opt}(t,x) \leq \bar{\rho}(t,x) - \beta \ , \\ \forall (t,x) \in [0;T] \times D, \ \beta \leq \rho_1^r(t,x) \ . \end{cases} \tag{69}$$

Then there exists an optimal couple (ρ_1^l, v_1^l) for L such that :

$$\begin{cases} \rho_1^r \underset{r \to 0}{\longrightarrow} \rho_1^l \text{ weakly} * \text{ in } L^\infty(Q) , \\ \\ v_1^r \underset{r \to 0}{\longrightarrow} v_1^l \text{ strongly in } L^2_{Loc}(Q) . \end{cases}$$

Proof : We know that ρ_r is uniformly bounded in $L^\infty(Q)$. We can then extract a subsequence converging weakly * in $L^\infty(Q)$ to a map ρ_l. From [5], we have the following lemma :

Lemma 4.7. *Let $(\rho_\alpha, m_\alpha = \rho_\alpha v_\alpha)$ be an optimal couple for L such that :*

$$\rho_\alpha(t,x) \geq r ,$$

a.e. for some constant $r > 0$. Then the kinetic energy

$$K = \frac{1}{2} \sum_\alpha \mu_\alpha \rho_\alpha |v_\alpha|^2 ,$$

is time-independent, and for every $\delta_0 \in]0; T/2[$, there is a constant $C = C(\delta_0)$ depending only on δ_0 such that

$$\int_{\delta_0}^{T-\delta_0} [|\nabla_x p| + \sum_\alpha \mu_\alpha \rho_\alpha (|\partial_t v_\alpha|^2 + |Dv_\alpha|^2)] \leq (1+K)C .$$

The kinetic energy of the solution of the minimization problem is clearly decreasing. We have then that $|v_\alpha^r|$, $|\partial_t v_\alpha^r|$ and $|Dv_\alpha^r|$ are uniformly bounded in $L^2_{Loc}(]0;T[, L^2(D))$. Thus, after extraction, v_α^r strongly converges to v_α^l in $L^2_{Loc}(]0;T[, L^2(D))$.

From $\partial_t \rho_\alpha^r + \nabla_x.(\rho_\alpha^r v_\alpha^r) = 0$, $\sum_\alpha \rho_\alpha^r = 1$, we have immediately :

$$\partial_t \rho_\alpha^l + \nabla_x.(\rho_\alpha^l v_\alpha^l) = 0, \ \sum_\alpha \rho_\alpha = 1 .$$

We have $\rho_r \geq \delta > 0$ a.e. in Q. We have :

$$L(\rho_r) \leq L_r(\rho_r) \leq L_r(\rho^{opt}) .$$

We take a solution of equation $\partial_t \tilde{\rho} + \nabla_x.\tilde{m} = 0$ in $L^2(Q)$ where $\tilde{\rho} = \bar{\rho} - \rho^{opt}$. Then since $\tilde{\rho} \geq \delta$, we have :

$$\int_0^T \int_D \frac{|\tilde{m}(t,x)|^2}{\tilde{\rho}(t,x)} dxdt \leq \frac{\|\tilde{m}\|^2_{L^2(Q)}}{\delta} = K \ .$$

We deduce that $L_r(\rho^{opt}) \leq L(\rho^{opt}) + rK$. We have now that (ρ_r, m_r) is a minimizing sequence for L.

Let $\epsilon > 0$. Since the kinetic energy is time-independent and the density ρ_1^r are uniformly bounded away from zero, we have :

$$\int_0^\delta \int_D |v_1^r(t,x)|^2 dxdt + \int_{[T-\delta;T]} \int_D |v_1^r(t,x)|^2 dxdt < 2\frac{\delta}{\beta} K \ .$$

We have then that for a δ small enough :

$$\int_0^\delta \int_D |v_1^r(t,x)|^2 dxdt + \int_{T-\delta}^T \int_D |v_1^r(t,x)|^2 dxdt < \epsilon \ . \tag{70}$$

We note $L^\delta(\rho, v) = \int_\delta^{T-\delta} \int_D \rho(t,x)|v(t,x)|^2 dxdt$. We have that for each r_0, r_1, r_2,

$$L^\delta(\rho^{r_0}, v^{r_1}) - L^\delta(\rho^{r_0}, v^{r_2}) \geq \|\bar{\rho}\|_{L^\infty} \ \epsilon \ .$$

From the strong L^2 convergence of v_r^1 to v_l^1 on the compact $[\delta, T-\delta] \times D$, we can fix a η such that for all $r > 0$, for all $0 < r_0, r_1 < \eta$,

$$\begin{aligned} |L^\delta(\rho_1^r, v_1^{r_0}) - L^\delta(\rho_1^r, v_1^{r_1})| \ &\leq \|\bar{\rho}\|_{L^\infty} (\|v_1^{r_0}\|^2_{L^2(Q_\delta)} - \|v_1^{r_1}\|^2_{L^2(Q_\delta)}) \ , \\ &\leq \|\bar{\rho}\|_{L^\infty} \epsilon \ . \end{aligned} \tag{71}$$

Since (ρ_1^r, v_1^r) is a minimizing sequence for L, there exists ν such that :

$$\forall 0 < r < \nu, \ |L(\rho_1^r, v_1^r) - I| \leq \epsilon \ . \tag{72}$$

We fix $r_0 < \eta$. From the weak convergence of ρ_1^r to ρ_1^l, we get :

$$\lim_{r \to 0} L^\delta(\rho_1^r, v_1^{r_0}) = L^\delta(\rho_1^l, v_1^{r_0}) \ . \tag{73}$$

From inequalities (70), (71), (72), and (73), we deduce that :

$$L(\rho_1^l, v_1^l) - I < (2 + 4 \ \|\bar{\rho}\|_{L^\infty(Q)})\epsilon \ . \tag{74}$$

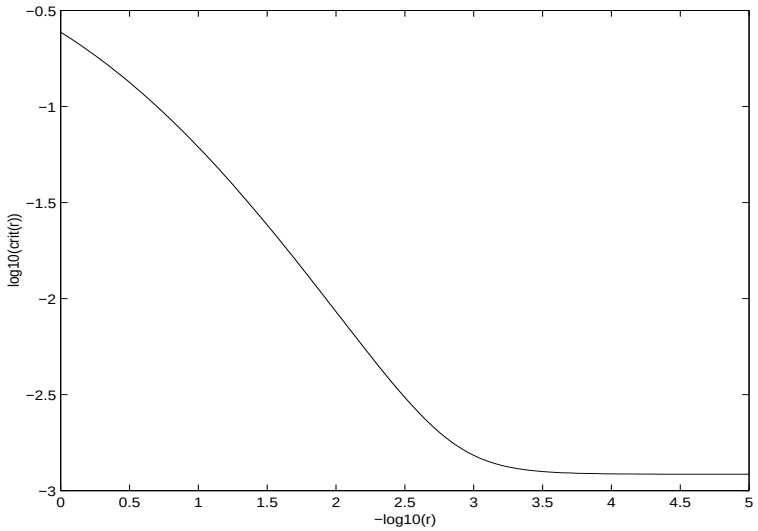

Figure 23: Convergence history

Thus we have that (ρ_1^l, v_1^l) is an optimal couple for the monophasic minimization problem. This completes the proof on theorem 4.6.

Remark : following some arguments of [5], we have the uniqueness of the optimal couple for L. Then we have the global convergence of the sequence (ρ_1^r, v_1^r) to $(\rho_1^{opt}, v_1^{opt})$.

Numerically, this convergence can be seen on figure 23. The densities used are the same as those used in subsection 4.1.3. When r is very small, the convergence saturates.

References

[1] V.I.Arnold, *Sur la géométrie différentielle des groupes de Lie de dimension infinie et ses applications à l'hydrodynamique, Ann. Institut Fourier 16 (1966) 319-361.*

[2] Y.Brenier, *The least action principle and the related concept of generalized flows for incompressible perfect fluids, J. Amer. Math. Soc. 2 (1989), no. 2, 225-255.*

[3] Y.Brenier, *Comm. Pure Appl. Math. 64 (1991) 375-417.*

[4] J.D. Benamou, Y.Brenier, *A numerical method for the optimal time-continuous mass transport problem and related problems, Contemp. Math. 226 (1999), 1–11*

[5] Y.Brenier, *A homogenized model for vortex sheets, Arch. Rational Mech. 138 (1997) 319-353.*

[6] Y.Brenier, *Homogeneous hydrostatic flows with convex velocity profiles, Nonlinearity 12 (1999) 495-512.*

[7] A. Shnirelman, *The geometry of the group of diffeomorphisms and the dynamics of an ideal incompressible fluid, Math. Sbornik USSR 56 (1987) 79-105.*

[8] A. Shnirelman, *Generalized fluid flows, their approximation and applications, Geom. Funct. Anal. 4 (1994), no. 5, 586-620.*

[9] L.A. Caffarelli, *Boundary regularity of maps with convex potentials. Ann. of Math. (2) 144 (1996), no. 3, 453–496.*

[10] R. McCann, (Mc) Duke Math. Journal 96 (ou 95) *Existence and uniqueness of monotone measure-preserving maps, Duke Math. J. 80 (1995), no. 2, 309–323.*

[11] W. Gangbo, R. J. McCann, *The geometry of optimal transportation, Acta Math. 177 (1996), no. 2, 113–161.*

[12] M. Cullen, R. J. McCann, *Free-boundaries and discontinuities in optimal transport, Communication at the workshop : 'Mathematics of atmosphere and ocean dynamics', Isaac Newton Institute, Cambridge, 1-5 December, 1997.*

[13] R. J. Douglas, *Decomposition of weather forecast error using rearrangements of functions, preprint.*

[14] M. Roesch, *Contributions à la description géomtriques des fluides parfaits incompressibles, Thèse de l'université Paris 6, 1995.*

[15] S. A. Kochengin, V. I. Oliker, *Determination of reflector surfaces from near-field scattering data, Inverse Problems 13, no. 2, 363–373, 1997.*

[16] Y. Brenier, E. Grenier, *Sticky particles and scalar conservation laws, SIAM J. Num. Anal, to appear.*

[17] J.-D. Benamou, *A domain decomposition method for the polar factorization of vector valued mappings, SIAM J. Num. Anal, 32:1808–1838, 1995.*

[18] F. Barthe *On a reverse form of the Brascamp-Lieb inequality, preprint 1997.*

[19] G. B.. Whitham, *Linear and nonlinear waves, Pure and Applied Mathematics. Wiley-Interscience John Wiley & Sons, New York-London-Sydney, 1974.*

[20] Y. Brenier, *Minimal geodesics on gropups of volume-preserving maps, tech. report ENS LMENS-9718, 1997.*

[21] D. Kinderlehrer, R. Jordan, F. Otto, *The variational formulation of the Fokker-Planck equation, preprint.*

[22] F. Otto, *Lubrication approximation with prescribed non-zero contact angle, preprint.*

[23] M. Fortin, R.Glowinski, *Augmented Lagrangian methods. Applications to the numerical solution of boundary value problems, Studies in Mathematics and its Applications, 15. North-Holland Publishing Co., Amsterdam-New York, 1983.*

[24] M.J.P. Cullen. Solution to a model of a front forced by deformation. *Q. J. R. Met. Soc.*, 109:565–573, 1983.

[25] M.J.P. Cullen. Implicit finite difference methods for modelling discontinuous atmospheric flows. *J. of Comp. Physics.*, 81:319–348, 1989.

[26] M.J.P. Cullen, J. Norbury, R.J. Purser, and G.J. Shutts. Modelling the quasi-equilibrium dynamics of the atmosphere. *QJR Meteorol. Soc.*, 113:735–757, 1987.

[27] M.J.P. Cullen and R.J. Purser. An extended lagrangian theory of semigeostrophic frontogenesis. *J. Atmos. Sci.*, 41:1477–1497, 1984.

[28] J.D. Benamou and Y.Brenier. Numerical resolution on a massively parallel computer of a test problem in meteorology using a domain decomposition algorithm. In North Holland, editor, *First European conference in computational fluid dynamics*, 1992.

Unit´e de recherche INRIA Lorraine, Technopôle de Nancy-Brabois, Campus scientifique,
615 rue du Jardin Botanique, BP 101, 54600 VILLERS LÈS NANCY
Unit´e de recherche INRIA Rennes, Irisa, Campus universitaire de Beaulieu, 35042 RENNES Cedex
Unit´e de recherche INRIA Rhône-Alpes, 655, avenue de l'Europe, 38330 MONTBONNOT ST MARTIN
Unit´e de recherche INRIA Rocquencourt, Domaine de Voluceau, Rocquencourt, BP 105, 78153 LE CHESNAY Cedex
Unit´e de recherche INRIA Sophia-Antipolis, 2004 route des Lucioles, BP 93, 06902 SOPHIA-ANTIPOLIS Cedex

Éditeur
INRIA, Domaine de Voluceau, Rocquencourt, BP 105, 78153 LE CHESNAY Cedex (France)
http://www.inria.fr
ISSN 0249-6399